Corso di dottorato di ricerca in:

"Scienze Biomediche e Biotecnologiche"

in convenzione con Centro di Riferimento Oncologico di Aviano, IRCCS

Ciclo 36°

Titolo della tesi

"ATG5 IN THE INDUCTION OF EPITHELIAL TO MESENCHYMAL TRANSITION"

Dottoranda

Giulia Tedesco

Supervisore

Dott.ssa Roberta Maestro

Co-supervisore

Dott.ssa Manuela Santarosa

Anno 2024

ABSTRACT

The reactivation of the embryonic epithelial-mesenchymal transition (EMT) program is a key step in tumor progression. In fact, this process has been associated with cellular migration and invasion, drug resistance and poor prognosis in various tumor contexts. In cancer, EMT is driven by the abnormal expression of specific embryonic transcription factors, including members of the SNAI, TWIST and ZEB families. However, the mechanisms that activate EMT transcription factors and the entire repertoire of molecules involved are still poorly characterized.

To identify novel mediators of EMT in cancer, it was performed in the laboratory a reverse-genetics screen based on a shRNA library infected in a triple-negative breast cancer model. The screen was thought to identify genes whose silencing resulted in an increment of epithelial features (E-cadherin re-expression). Interestingly, a number of autophagy genes were isolated, and particularly ATG5.

Autophagy is a conserved degradation pathway, usually triggered by nutrient deprivation, that removes unnecessary or dysfunctional components through a lysosome-dependent mechanism. Numerous studies link autophagy activation in tumors with the development of typical EMT features, such as the acquisition of a motile and invasive phenotype. Furthermore, activation of autophagy in established and metastatic tumors is often associated with poor patient survival.

On this ground, we assessed the translational significance of ATG5 expression analyzing ATG5 levels in a series of primary breast tumors obtained from the TCGA BRCA project. We found that ATG5 levels are significantly increased in the basal and HER2 breast cancer subgroups compared to luminal cancers and that high ATG5 expression is associated with poorer prognosis in a group of luminal B breast cancer patients.

To investigate the molecular mechanism involving ATG5 in EMT, we performed an interactome study based on affinity purification combined with an LC-MS/MS technique. Our previous data suggested a possible autophagy-independent role of ATG5 in the induction of EMT, so the proteomic study was performed using cells overexpressing an autophagy-deficient form of ATG5 (ATG5K130R mutation). This mutant allowed us to focus our attention on a number of non-autophagic interactors of ATG5, which included the ubiquitin ligase KEAP1. The interaction between ATG5 and KEAP1 was confirmed using an affinity purification method and a proximity ligation assay (TurboID). We also observed that downregulation of ATG5 can increase the level of NRF2 protein, a transcription factor that is negatively regulated by KEAP1. Furthermore, ATG5 downregulation determines the upregulation of NRF2 downstream targets. Taken together, the results collected here suggest an unconventional role

of ATG5 through its interaction with KEAP1. We propose that ATG5 might act on NRF2 activity via KEAP1 and subsequently influence the activation of NRF2 downstream targets. This activation could affect the aggressiveness of breast cancer.

INDEX

1. INTRODUCTION

1.1 EPITHELIAL TO MESENCHYMAL TRANSITION

Epithelial to mesenchymal transition (EMT) is a physiological program involved in embryogenesis and wound healing. During EMT, polarized cells undergo epigenetic and transcriptional changes that lead to decreased expression of epithelial adhesion molecules and increased expression of mesenchymal factors. These modifications determine cytoskeletal rearrangements in cells and the secretion of extracellular matrix proteases producing substantial morphological changes in tissues (Zeisberg & Neilson, 2009).

EMT can be categorized into three different types based on their biological functions (Fig. 1). According to pioneering studies conducted in chicken embryos, type I EMT (embryonic EMT) is essential for the acquisition of migratory capacity and the formation of mesoderm and neural crest (M A Nieto et al., 1994). Type II EMT is a process that is activated in adult tissues for wound healing. The transient activation of EMT allows keratinocytes to become motile and reach the damaged area to restore the epidermal barrier (Kalluri & Weinberg, 2009). Type III EMT is specific to neoplastic tissue. Reactivation of EMT has an important role in cancer progression, as EMT can confer metastatic properties to tumor cells and enhance invasion allowing the colonization of surrounding tissues and distant organs (Huang et al., 2022).

In recent years it has been observed that EMT is rarely fully executed in tumor cells. The simultaneous expression of epithelial adhesion molecules and EMT transcription factors that support metastasis through a partial EMT program was recently observed in patient-derived breast cancer xenografts (Saini et al., 2023)

In an in vivo mouse model, the injection of partially mesenchymal cells of skin squamous cell carcinoma produced more metastasis than using fully mesenchymal cells (Pastushenko et al., 2018). Genomic and functional studies have further shown that co-expression of epithelial and mesenchymal markers occurs in disseminated cancer cells (Aiello et al., 2018; Pastushenko et al., 2021; Puram et al., 2017). For example, the deletion of FAT1, a gene coding for a protocadherin, promotes the acquisition of a hybrid EMT state that presents increased tumour stemness and metastasic potential (Pastushenko et al., 2021). Moreover, partial EMT may rely on an altered intracellular trafficking of E-cadherin and other epithelial proteins allowing tumor cells to retain associative properties for collective migration (Aiello et al., 2018).

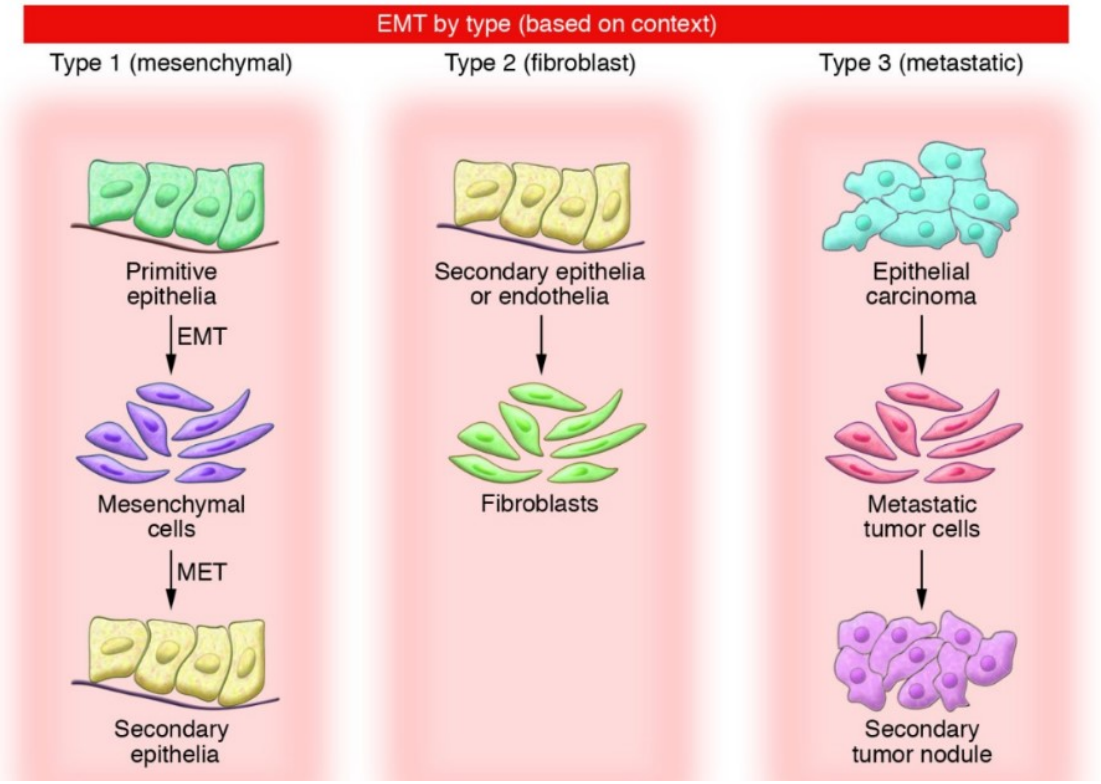

Figure 1. Schematic representation of the three types of Epithelial to Mesenchymal transition. Adapted from Zeisberg and Neilson, 2009

1.1.1 MARKERS OF EPITHELIAL AND MESENCHYMAL STATUS

The invasiveness of cancer cells is based on the acquisition of motility and mesenchymal characteristics that depend on the alteration of cellular junctions involved in cell-cell contacts and cell-extacellular matrix (ECM) contacts (Santarosa & Maestro, 2021) (Fig. 2).

Adherens junctions control cell-cell adhesion and are based on the homophilic interaction of cadherins. Cadherins are a family of transmembrane proteins that are localized at the apicobasal interface of cells and associate by their intracellular domains with diverse regulatory and cortical proteins, such as α-, β-, γ-, and p120-catenin, actinin, and vinculin (Ivanov & Naydenov, 2013; Santarosa & Maestro, 2021). Different cadherin isoforms are expressed in a tissue-specific manner and they show structural divergences. Type I cadherins include E-cadherin (epithelial cadherin) and N-cadherin (neuronal cadherin). E-cadherin is expressed in all epithelial tissues and it forms homophilic bonds between the adherens junctions

on the surface of epithelial cells ensuring the maintenance of epithelial contacts (van Roy, 2014).

N-cadherin is highly expressed in non-epithelial tissues. In cancer, abnormal N-cadherin expression by epithelial cells favors the formation of heterotypic adhesion complexes between epithelial cells and stromal cells, which typically express N-cadherin. This interaction favors the migration and invasion of cancer cells (van Roy, 2014).

Adhesion molecules are functionally linked to the internal cell structure, constituted by the actin cytoskeleton network. Epithelial cells mainly use cytokeratin intermediate filaments to build the actin cytoskeleton, whereas mesenchymal cells primarily rely on vimentin (Kuburich et al., 2022). Vimentin is a protein that forms coiled-coiled homotetramers to build intermediate filaments and is recruited to the cellular membrane by directly binding to integrin β3 (J. Kim et al., 2016). Moreover vimentin is involved in the formation of focal adhesions (Kuburich et al., 2022), which are junctions specialized in the interaction between the cell and the ECM. The main components of the focal adhesions are integrins, which are $\alpha\beta$ heterodimers that regulate cell–matrix and cell–cell interactions (Kuo, 2014).

The interaction between cancer cells and the ECM also involves changes in the ECM structure. Fibronectin 1 (FN1) is a scaffold glycoprotein involved in ECM fibrillogenesis. It is a key element for integrin-mediated signaling and is mainly produced by fibroblasts (Rick et al., 2019). Cancer cells are able to produce FN1 and influence the tumor microenvironment towards pro-survival signaling (Barbazán et al., 2017; Montagner et al., 2020; Rick et al., 2019). The

FN1-rich ECM is indeed able to promote cancer cells survival by influencing the availability of growth factors and cytokeratins or by controlling TGFβ/TNFα signaling (Spada et al., 2021)

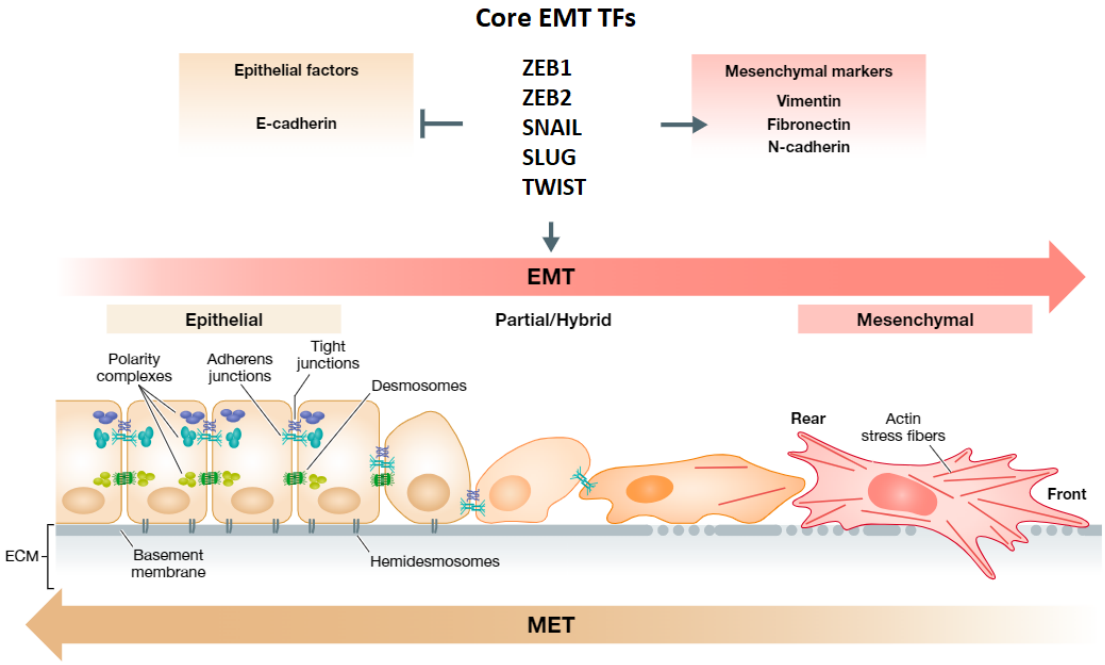

Figure 2. EMT program outline. Phenotypic variations, markers and transcription factors associated with EMT. Adapted from Brabletz et al. 2021

1.1.2 EMT TRANSCRIPTION FACTORS

The key players in EMT are the EMT transcription factors (EMT-TFs) which are normally active during embryonic development but are abnormally reactivated in the neoplastic context (Stemmler et al., 2019). EMT-TFs are the driving forces behind the changes that influence the morphology and behavior of cancer cells. EMT-TFs include members of the SNAI, TWIST and ZEB families. SNAI and ZEB belong to the zinc finger transcription factor family, while TWIST belongs to the basic helix-loop-helix family.

SNAI, ZEB and TWIST are transcriptional repressors that are able to directly bind to the promoters of target genes (e.g. E-cadherin) and repress the expression of epithelial markers (Bolós et al., 2003; Canel et al., 2013; Puisieux et al., 2014; Vesuna et al., 2008). In addition, EMT-TFs are able to form transcription complexes and act as transcriptional activators for mesenchymal genes (Skrypek et al., 2017). EMT-TFs are also able to exert a long-lasting effect on genes expression by cooperating with epigenetic remodelers that act on DNA methylation and histone modification (Gupta et al., 2019).

Members of the SNAI family can inhibit the expression of CDH1 (the E-cadherin coding gene) by binding directly to the E-box (5'-CANNTG-3') localized in its promoter (Hajra et al., 2002). In addition, SNAI family members carry a SNAG domain capable of recruiting the Polycomb Repressor Complex 2 (PRC2), which induces repressive histone modifications (H3/H4 deacetylation, H3K4 demethylation, and H3K9 and H3K27 hypermethylation) and repressive DNA methylation in cooperation with DNMTs (Chiang & Ayyanathan, 2013). On the other hand, SNAI1 acts as a transcriptional activator that interacts with EGR-1 and SP1 and activate transcription of MMP9, moreover both SNAI1 and SNAI2 induce ZEB1 (Wu et al., 2017).

Similar to SNAI, ZEB1 represses transcription of the CDH1 gene by binding its E-box and recruiting epigenetic modifiers (CtBP and PRCs) as well as recruiting the SWI/SNF chromatin remodeling complex BRG1. ZEB1 recruits histone deacetylases (HDAC) for transcriptional repression (Aghdassi et al., 2012; Sánchez-Tilló et al., 2010; Shi et al., 2003). ZEB1 can also act as a transcriptional activator for various mesenchymal genes, including collagen, smooth muscle actin, vimentin and N-cadherin (Dongre & Weinberg, 2019).

TWIST1 transcription factor forms dimers to the E-box of target genes to repress their transcription and it is able to recruit epigenetic remodelers (MTA2, RbAp46, Mi2 and HDAC2) that block the expression of CDH1 (Fu et al., 2011). TWIST1 can also bind and inhibit the activity of a number of TFs (MYOD, RUNX1, RUNX2) finally blocking differentiation (Bialek et al., 2004; Hamamori et al., 1997; Sharabi et al., 2008; Spicer et al., 1996) or inhibit p53 tumor suppressive function (Shiota et al., 2008) . TWIST1 positively regulates SNAI2 expression (Casas et al., 2011) and cooperates with SNAI1 for the transcriptional induction of ZEB1 (Dave et al., 2011). Moreover, TWIST1 has been shown to induce transcription of CDH2 the (N-cadherin gene) by binding to the transcription E-box cis-element located within the first intron of the N-cadherin gene (Alexander et al., 2006).

EMT-TFs are involved in cross-regulatory mechanisms with miRNAs (Fig.3). ZEB1 activity is regulated by miR-200 family (miR-200f). Analyzing the miRNA expression profile analyses of 60 epithelial and mesenchymal cell lines from the National Cancer Institute it was observed a significant positive correlation between high E-cadherin and miR-200f levels (Park et al., 2008). Consistently, in breast cancer models, downregulation of miR-200c is associated with increased ZEB1 expression and metastasis (Damiano et al., 2017). ZEB1 can also be negatively regulated by miR-130 (Dong et al., 2013). Other regulatory loops involving miRNAs exist between SNAI1, and the miR-34f (miR-34a, miR-34b, and miR-34c) and between SNAI1 and miR-203 (Moes et al., 2012; Siemens et al., 2011). SNAI1-dependent EMT is activated in

colon, breast, and lung carcinoma cells as a consequence of a decrease in miR-34 levels (N. H. Kim et al., 2011). SNAI1 and ZEB1 directly repress the miR-34f and miR-200f promoters, respectively, providing a tight crosstalk between the ZEB/miR-200 and SNAI1/miR-34 pathways (Bracken et al., 2008; Burk et al., 2008; Siemens et al., 2011).

Increasing evidence suggests that EMT-TFs act in a tumor-specific manner. For example, in mouse models of pancreatic cancer, it was found that deletion of SNAI1 or TWIST1 does not affect tumor progression (Zheng et al., 2015). Conversely, knocking out ZEB1 in the same model leads to a reduction in pre-neoplastic and neoplastic lesions and a reduction in tumor aggressiveness (Krebs et al., 2017). Moreover, in renal cell carcinoma, TWIST1 is the only EMT-TF associated with poor patient outcome (Harada et al., 2012).

As previously reported, cells undergoing EMT become invasive and acquire resistance to treatments. In particular, ZEB1, SNAI1 and SNAI2 confer resistance to oxaliplatin and cisplatin in different tumor contexts (Lim et al., 2013). An association between EMT and resistance to gemcitabine was observed in both pancreatic cancer patients and mouse models (Zheng et al., 2015).

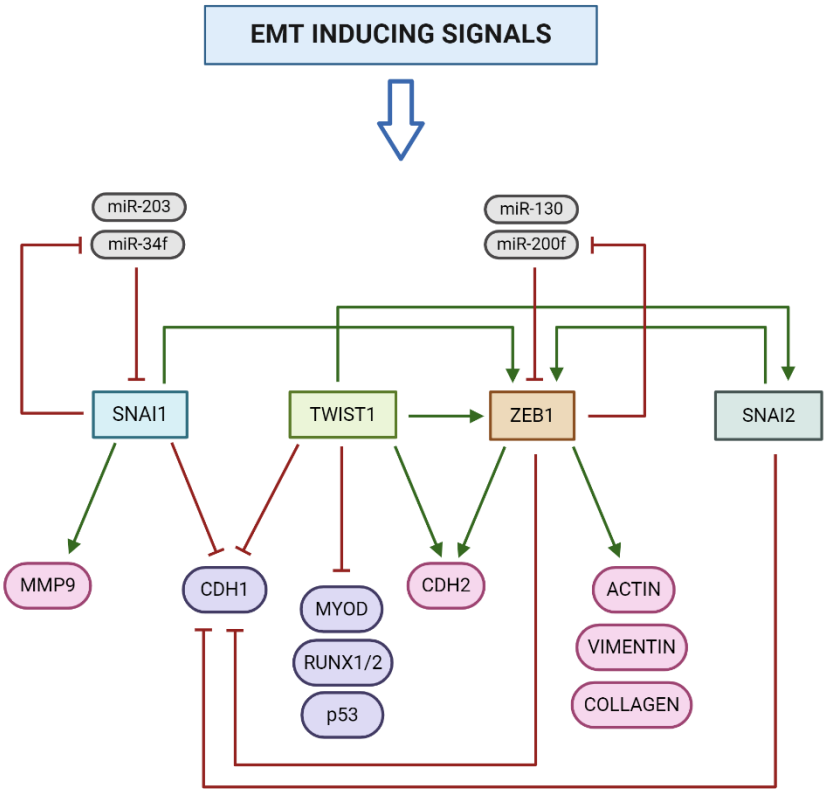

Figure 3. The complex transcriptional regulatory network of EMT transcription factors. EMT-TF are hallmarked by colored squares, pink identifies genes with pro-EMT functions, purple identifies those genes with anti-EMT functions. Created with Biorender.com

1.2 AUTOPHAGY

Autophagy is a catabolic process conserved from yeast to humans that is responsible for the degradation and recycling of cellular components. Autophagy can be either non-selective or selective in the removal of molecules, and the mechanisms behind the selectivity of the process are currently not fully understood (Gatica et al., 2018). The metabolites derived from the autophagic process are used by the cell as an energy source to overcome bioenergetic shortage or as building blocks to regenerate components of survival pathways (respiratory chain proteins and antioxidant enzymes) (Noboru Mizushima & Komatsu, 2011). Autophagy is broadly engaged in physiology. This process is also used by cells to react against environmental stresses such as intracellular pathogens assault. On the other side autophagy deregulation is involved in pathologies as neurodegeneration, and cancer (Reggiori & Klionsky, 2013).

There are three main types of autophagy, each serving distinct functions within the cell (Fig. 4). Macroautophagy is a catabolic process that involves the formation of a double-membrane structure called the autophagosome, which engulfs cytoplasmic contents including proteins, organelles, and other cellular debris. The autophagosome then fuses with lysosomes, forming an autolysosome, where the engulfed material is degraded by lysosomal enzymes. (Feng et al., 2014).

In microautophagy, small parts of the cytoplasm or organelles are directly engulfed by invaginations of the lysosomal membrane. This leads to degradation of the engulfed material within the lysosome. Microautophagy is considered a non-selective process that does not specifically target particular components for degradation. Instead, it provides a mechanism for the bulk degradation of cytoplasmic contents and thus contributes to the maintenance of cellular homeostasis. While macroautophagy involves the formation of autophagosomes and subsequent fusion with lysosomes, microautophagy bypasses the intermediate step of autophagosome formation and results in direct uptake of cargo by the lysosome (Fernández-Albarral et al., 2021; W. Li et al., 2012).

Chaperone-mediated autophagy (CMA) is a selective form of autophagy in which certain proteins are specifically degraded. Proteins to be degraded by CMA contain a specific recognition motif, the KFERQ motif, which is recognized by cytosolic chaperone proteins (HSC70). These chaperones then transport the target proteins to the lysosomal membrane, where they are translocated to the lysosome for degradation (Kaushik & Cuervo, 2018).

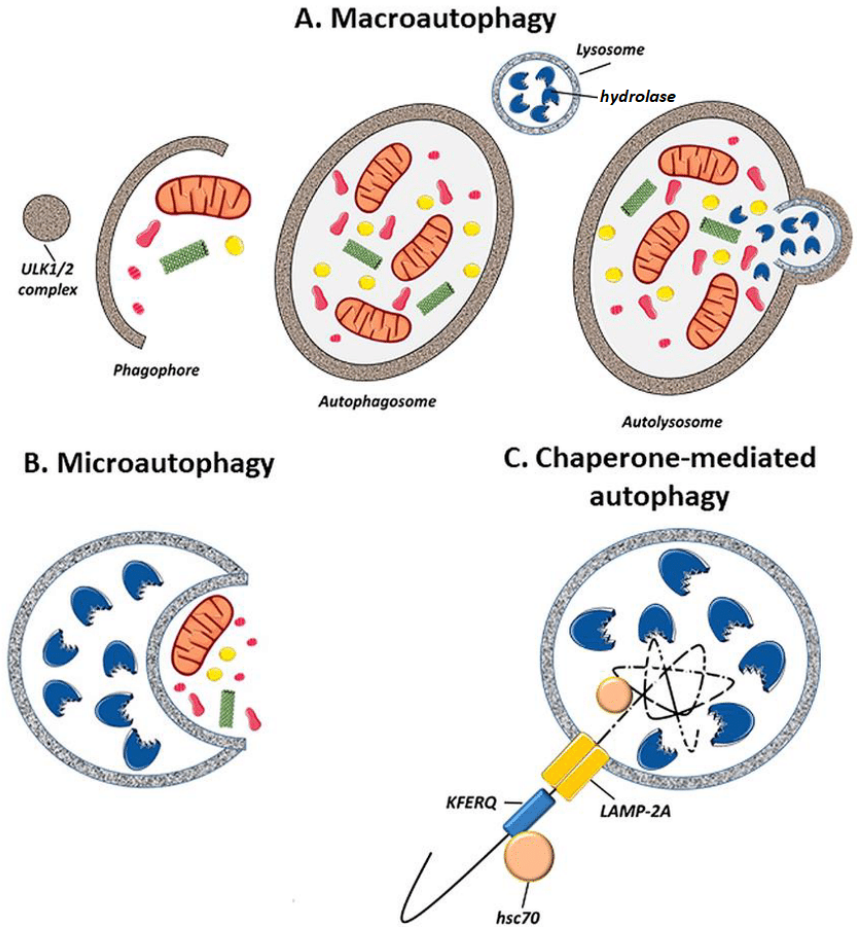

Figure 4. Main autophagic pathways (A) Macroautophagy, (B) Microautophagy, (C) Chaperone Mediated autophagy. Adapted from José A. Fernández-Albarral et al. 2021

.

1.2.1 THE MACROAUTOPHAGY CASCADE

Macroautophagy, hereafter referred to as autophagy, is a finely regulated event. The first group of about 20 molecules, called autophagy-related genes, was discovered by pioneering studies in yeast where these core molecules were identified for their involvement in several phases of the autophagy process (Kuma et al., 2004; Levine & Kroemer, 2019). Then, the group of autophagic molecules was further investigated in various organisms including humans.

Currently, the BioGRID Autophagy Project reports information on about 200 human proteins functionally involved in autophagy (https://thebiogrid.org/project/6/autophagy.html) (Oughtred et al., 2021).

Autophagy progression involves five steps: initiation, nucleation, elongation, autophagosome-lysosome fusion and substrate degradation (Fig. 5). The first step of autophagy, initiation, starts with the formation of the assembly site in a region proximal to ER called, in yeast, phagophore assembly site (PAS) (Dikic & Elazar, 2018). In the nucleation phase the assembly site is the center of the formation of a double membraned structure that expands gradually to form an open vesicle, the phagophore. Once the material is incorporated, the double membraned structure seals forming a vesicle named autophagosome. Further stimuli drive the autophagosome towards fusion with the lysosome and the process ends with lysosome-mediated degradation of the cargo (Noboru Mizushima et al., 2011).

One of the key sensors of energy, nutrient and redox status is the mTORC1 protein complex, which consists of the Ser/Thr kinase mTOR and other regulatory components (Agarwal et al., 2015). Under nutrient-limited conditions, the amount of ATP decreases and the increased AMP/ATP ratio triggers the activation of AMPK, which in turn restrains mTORC1 and its inhibitory activity towards ULK1. When mTOR is blocked ULK1 is activated and initiates the autophagy cascade (Hosokawa et al., 2009). ULK1 complex (comprising the ULK1, ATG101, FIP200/RB1CC1 and ATG13 proteins) phosphorylates some of the components of the PI3K complex I (formed by PIK3C3, Beclin-1, ATG14 and VPS15/PIK3R4) eventually activating PIK3C3 subunit. PIK3C3 is a phosphatidylinositol-3-kinase that phosphorylates phosphatidylinositol (PI) to produce phosphatidylinositol-3-phosphate (PI3P) (Yuan et al., 2013). PI3P is fundamental for the nucleation phase of autophagy: it is placed on the nascent phagophore membrane and gives rise to the phagophore. PI3K complex can be positively regulated by UVRAG (UV radiation resistance-associated gene) and the autophagy and AMBRA1 (beclin 1 regulator 1) (Fimia et al., 2007). The phagophore constitutes the substrate

for the following assembly of the phagophore elongation complexes. These events are supported by ATG9, a lipid scramblase incorporated into vesicles and involved in nucleation which may deliver additional lipids and proteins contributing to membrane expansion (Chang et al., 2021), furthermore ATG2 seems to be involved in providing lipids to the elongating phagophore from donor structures, like ER (Matoba et al., 2020).

PI3P is recognized by scaffold proteins which recruit two ubiquitin-like conjugation systems on the nascent phagophore: ATG5-ATG12-ATG16L1 and microtubule-associated protein 1-light chain 3 (MAP1LC3 or LC3) (Itakura & Mizushima, 2010).

The ATG5-ATG12-ATG16L1 complex is formed by a reaction cascade involving ATG7 (E1-like enzyme) and ATG10 (E2-like enzyme), which mediate covalent binding between ATG5 and ATG12. Subsequently, the ATG5-ATG12 conjugate binds ATG16L1 and forms a ternary complex located at the phagophore membrane (Dooley et al., 2014). Recent studies propose an alternative model for the formation of ATG5:ATG12-ATG16L1 complex. Based on the proposed model an interaction between ATG5 and ATG16L1 is needed first, this interaction forms a transient ATG5-ATG16L1 doublet that allows the recruitment of ATG12 and the final formation of a stable trimeric structure based on the covalent binding between ATG12 and ATG5 (Baines et al., 2022; Haller et al., 2014; Wible et al., 2019).

LC3 processing occurs at the same time of ATG5:ATG12-ATG16 complex formation. The ATG5-ATG12-ATG16L1 complex serves as a scaffold and promotes LC3 lipidation (Dooley et al., 2014). LC3 (or MAP1LC3) is the ortholog of Atg8 in yeast. LC3 is first cleaved at its carboxy terminus by ATG4 to form LC3 I. Following ATG4-mediated cleavage, LC3 is activated by ATG7 (E1-like enzyme) and ATG3 (E2-like enzyme) and finally conjugated to phosphatidylethanolamine (PE) to form the active LC3 (LC3-II) (Tanida et al., 2004). The ATG5:ATG12-ATG16L1 complex together with LC3-II fosters autophagic membrane elongation and phagophore expansion. Phagophore growth also needs the support of newly synthetized lipids, so metabolism machinery becomes devoted to lipid synthesis in starving conditions, however how these changes are regulated is currently unknown (Melia et al., 2020).

Autophagic membrane elongation goes along with cargo sequestration during phagophore expansion. Cargo sequestration is a complex event that can be mediated by specific receptors. Cargo receptors regulate the localization and the identification of the structures to be degraded, one of the main cargo receptors is Sequestrosome-1 (SQSTM1) (Lamark & Johansen, 2021; Pankiv et al., 2007). Autophagy receptors are molecules that selectively identify specific cellular organelles. These molecules can be both soluble and membrane bound and include, for

example, RETREG1 and RTN3 that are selectively recognized by the autophagy system (Grumati et al., 2017; Khaminets et al., 2015).

In the late stages of the autophagic process, the phagophore closes and fuses with the lysosome to form the phagolysosome. This phase relies on soluble SNARE proteins, which are found in both membranes (Yim & Mizushima, 2020). The activity of the two known SNARE complexes (TX17-SNAP29-VAMP7/VAMP812 and STX7-SNAP29-YKT6 complexes) is facilitated by the tethering factors such as the HOPS complex, PLEKHM1 and EPG5, which promote the close interaction between the membranes.

In the phagolysosome, acid hydrolases degrade the autophagic bulk generating metabolites that stream out through transporters and channels (Dikic & Elazar, 2018). The nutrients obtained through the autophagy pathway stimulate the activation of mTOR. mTOR consequently inhibits the autophagic stimulus phosphorylating ULK1, ATG13 and UVRAG. At the end a negative feedback mechanism stops autophagy (Shin & Zoncu, 2020; Wong et al., 2018; Yu et al., 2010).

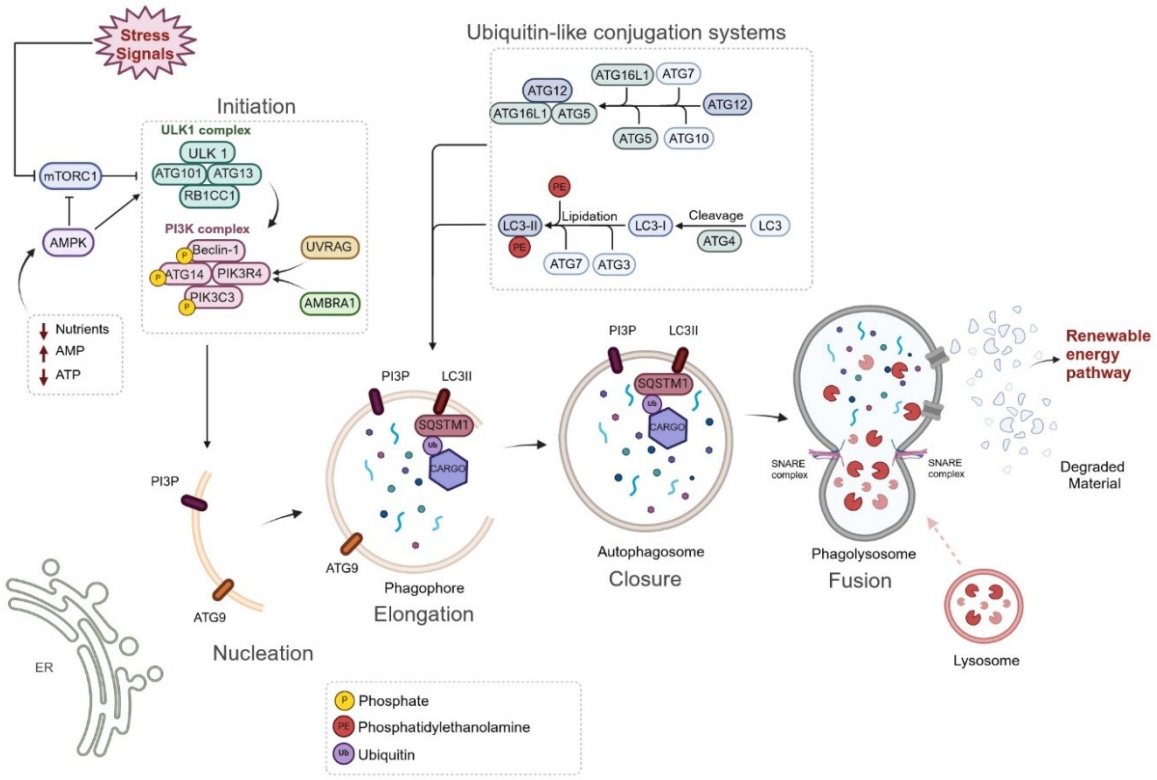

Figure 5. Illustration of the main phases of autophagy, from the formation of the phagophore to fusion with the lysosome, which involves the degradation of autophagic cargo by lysosomal proteases. Created with Biorender.com

1.2.2 AUTOPHAGY AND CANCER

Autophagy plays a dual role in cancer by being both a pro-tumoral and a tumor suppressive process (J. Y. Guo et al., 2013). Indeed, in the early stages of neoplastic progression, autophagy can prevent the onset of tumors by eliminating toxic protein aggregates and damaged organelles. On the other side, in advanced tumoral stages, it can play a tumor-promoting role by providing the nutrients necessary for cancer cell metabolism for their growth and survival (White, 2012).

A dual and context-dependent role of autophagy in cancer appears to be closely linked to the genetic background of the neoplasm, as shown in genetically modified mouse models of pancreatic cancer, where the pro-tumorigenic role of autophagy appears to be related to p53 deficiency (A. Yang et al., 2018).

Dependence on autophagy is a common feature of numerous advanced tumors (X. Li et al., 2020). This process is often associated with aberrant reactivation of epithelial-mesenchymal transition (EMT), leading to downregulation of cell-cell and cell-basement membrane interactions and metastatic dissemination of tumor cells (M Angela Nieto et al., 2016; Vera-Ramirez, 2020). Indeed, numerous studies have shown a positive correlation between autophagy and EMT. In particular, several experimental models have described that autophagy supports the survival and metastatic dissemination of tumor cells that have acquired EMT-like properties and drug resistance (Gugnoni et al., 2016; Sakuma et al., 2016). In addition, activation of autophagy by starvation appears to induce the TGFβ/SMAD3 signaling pathway, which is commonly associated with activation of the EMT program (Vera-Ramirez, 2020). Autophagy is also involved in the regulation of EMT-TFs. In both mouse embryonic fibroblasts and human tumor cell lines, p62/SQSTM1 mediates TWIST1 and SNAI1 stabilization, leading to the acquisition of malignant properties. In addition, overexpression of p62/SQSTM1, a common feature of various carcinomas, is associated with the EMT and metastasis and is considered a negative prognostic factor for patients (Qiang et al., 2014).

1.2.3 ATG5 IN AUTOPHAGY AND NON AUTOPHAGIC PROCESSES

The formation of the autophagosome is the most critical step in autophagy. In this process ATG5, together with ATG12 and ATG16L1, is involved in autophagosome formation, as mentioned above.

The crystal structures of human ATG5-ATG12 conjugated with a short N-terminal peptide of ATG16 revealed the structure of this trimeric complex (Fig. 6). ATG5 contains two ubiquitin-like domains connected by a helix-rich domain, and ATG16 binds the ubiquitin-like domains of ATG5. ATG12 interacts with ATG5 on the opposite side to ATG16 and there are no contacts between ATG12 and ATG16. The complex between ATG5 and ATG12 is determined by a covalent bond between ATG5 Lys130 and ATG12 Gly140 (Otomo et al., 2013). Indeed, an autophagy deficient form of ATG5 carrying a substitution of Lys130 with an Arg (ATG5K130R) is frequently used to prevent ATG5:ATG12 covalent binding (N Mizushima et al., 1998). Furthermore, ATG5 and ATG12 interact via extensive hydrophobic and hydrophilic interactions (Changotra et al., 2022; Chew & Yip, 2014; Otomo et al., 2013).

While ATG5 primarily plays a role in autophagy, recent studies suggest that it may have additional functions beyond this process.

Together with ATG16L1, ATG5 is also able to control membranes for exosome production and induce the release of known invasion mediators (RAS, β-catenin and vimentin) and ultimately promote invasion and metastasis of breast cancer cells in mice (H. Guo et al., 2018).

In addition, ATG5 is involved in apoptosis. It can be specifically cleaved by calpains (CALPAIN1/2), and truncated ATG5 can translocate to the mitochondria, associate with Bcl-2-like protein 1 (BCL2L1), and trigger caspase activation via an autophagy-independent mechanism (Yousefi et al., 2006).

ATG5 can translocate to the nucleus where it interacts with Mis18α, a centromeric protein involved in chromatin methylation. ATG5-Mis18α binding increases MLH1 promoter methylation (a component of DNA mismatch repair) and thereby enhances mismatch repair defects and resistance of colorectal cancer patients to 5-fluorouracil (Sun et al., 2021). Furthermore, ATG5 is able to interact with BIRC5 to induce mitotic catastrophe independent of autophagy (Maskey et al., 2013).

In various solid tumors high ATG5 expression has been associated with poor patient prognosis (Hu et al., 2021; Xu et al., 2021). ATG5 has been suggested as a potential prognostic marker in

cervical squamous cell carcinoma and endocervical adenocarcinoma from the Cancer Genome Atlas (S. Zhou et al., 2021).

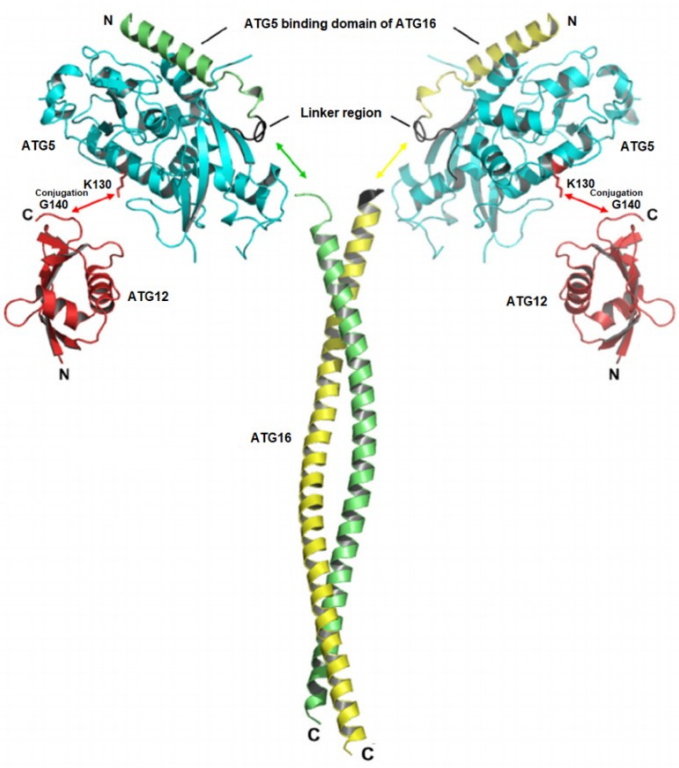

Figure 6. Proposed model of the Atg12-Atg5 and Atg16 complex. Atg5 and Atg12 are colored cyan and red, respectively. The two Atg16 molecules are colored green and yellow, and the linker regions are black. Adapted from Fujioka et al. 2009

1.3 BREAST CANCER

Breast cancer is the most common type of cancer in women. In 2020, more than 2 million new cases were diagnosed worldwide (Sung et al., 2021). Breast cancer refers to an heterogeneous group of tumors characterized by strong variability in morphologic and biological features, thus these tumors show different clinical behavior and response to treatments (Tsang & Tse, 2020). Breast cancer can be classified according to histopathological features, genetic alterations or gene expression profiles (Kreike et al., 2007). Cancer classification aims to provide an accurate diagnosis of the disease and prediction of tumor behavior to facilitate oncologic decision making.

From an histologic point of view breast cancer can be classified as invasive ductal carcinoma and invasive lobular carcinoma mainly. Other less common histologic types are mucinous, cribriform, micropapillary, papillary, tubular, medullary, metaplastic, and apocrine carcinomas. Infiltrating ductal carcinomas account for 70% to 80% of all invasive breast cancers, however these tumors may show highly heterogeneous biological behavior (Tsang & Tse, 2020). This indicates that histologic typing represents a broad categorization that may not capture the peculiar clinical courses of individual breast cancers.

In the early 2000s, studies have focused on refining breast cancer classification using information from high-throughput technologies. Gene expression studies have made it possible to categorize breast tumors based on their transcriptional profile: Luminal A, Luminal B, HER2-enriched, Normal-like and Basal-like (Sørlie et al., 2001).

The subtypes Luminal A and Luminal B are the most common groups. The term "luminal" refers to the lumen, the inner empty space formed by alveoli and ducts. The cells forming those structures are influenced by estrogen and progesterone for their development. Indeed, Luminal A and Luminal B subgroups are characterized by the expression of ER and/or PR. Treatment with anti-estrogens and aromatase inhibitors ensures a high survival rate for these patients (Lambertini et al., 2015; Matsumoto et al., 2015; Orrantia-Borunda et al., 2022). HER2-enriched tumors are characterized by amplification of the HER2 gene.

The normal-like cluster was initially defined by expression of genes similar to normal breast epithelium. However, it is a controversial subgroup and has been later considered to be an artifact due to normal epithelial cells contamination (Weigelt et al., 2010).

Finally, basal-like tumors are characterized by an increased expression of basal cytokeratins (e.g. CK5/6 and CK14) (Gazinska et al., 2013).

The molecular subgrouping determined the possibility to develop a new prognostic tool, PAM50. PAM50 is a standardized method that categorizes breast cancers into luminal A, luminal B, HER2-enriched, and Basal breast cancer using a 50 genes signature that can be applied to gene expression derived from microarrays, RNASeq, or qRT-PCR. A modified version of PAM50, Prosigna, has become a test approved by US Food and Drug Administration, for the prognosis of postmenopausal hormonal receptor–positive breast cancer patients. Prosigna shows predictive value for recurrence and benefit of adjuvant chemotherapy (Tsang & Tse, 2020).

From an immunohistochemical perspective breast cancer can be classified based on the expression of three receptors: the estrogen receptor (ER), the progesterone receptor (PR) and the receptor for human epidermal growth factor 2 (HER2). These receptors are used as prognostic markers and important predictive factors for hormonal and anti-HER2-targeted therapy. ER and PR are nuclear sex steroid receptors that stimulate the growth of normal and neoplastic breast epithelium. They are expressed in almost 75% of all breast cancers. When present, they are indicators for responsiveness to hormonal therapy (Waks & Winer, 2019) .

Approximately 15% of breast cancers overexpress HER2 with amplification of the gene located at 17q12 (Lesurf et al., 2017). Although these tumors are inherently aggressive, they may benefit from therapies that target HER2, such as trastuzumab or lapatinib (Molina et al., 2001). The remaining part of tumors characterized by the lack of expression of these receptors, are defined as Triple-negative breast cancers (TNBC) TNBC are in general high grade and associated with a poor prognosis. Patients with TNBC do not benefit from targeted therapies (Orrantia-Borunda et al., 2022).

TNBCs mainly affect young premenopausal women (under 40 years of age) and account for about 15-20% of all breast cancer cases. The survival time of patients with TNBC is shorter than that of patients with other breast cancer subtypes: the mortality rate is 40% within the first 5 years after diagnosis and about 46% develop distant metastases (Yin et al., 2020). There is a link between the basal type of breast cancer and mutations in the BRCA genes, key molecules involved in DNA damage repair. In fact, about 10-20% of TNBCs occur in patients carrying germline mutations in BRCA1 (Tutt et al., 2018). TNBC is the most common histotype of breast cancer in this patient cohort (Gonzalez-Angulo et al., 2011). As confirmed by the cancer genomics program Cancer Genome Atlas Network (TCGA) that includes a large number of primary breast tumors, TNBCs are characterized by a high frequency, around 80%, of inactivating mutations in the TP53 tumor suppressor gene (Cancer Genome Atlas Network,

2012). Analysis of gene expression profiles allowed the identification of 6 distinct subgroups of TNBC that may be considered to suggest new targeted molecular therapies (Lehmann et al., 2011).

A characteristic feature of TNBC and basal-like tumors is the manifestation of an EMT phenotype characterized by increased expression of mesenchymal markers and low residual expression of epithelial markers (Kvokačková et al., 2021). It is assumed that this phenotype as EMT or partial EMT contributes significantly to the aggressiveness of TNBC. In addition, there is increasing evidence that abnormal activation of the autophagic pathway also plays an important role in determining the clinico-biological characteristics of these tumors (Grandvallet et al., 2020).

1.4 KEAP1 AND THE CONTROL OF NRF2 TRANSCRIPTION FACTOR STABILITY

The KEAP1-NRF2 (Kelch-like ECH-associated protein 1-Nuclear factor erythroid 2-related factor 2) axis is a crucial signaling pathway involved in cellular defense against oxidative stress. This pathway plays a significant role in maintaining cellular redox homeostasis and protecting cells from damage caused by reactive oxygen species (ROS). Dysregulation of the KEAP1-NRF2 axis has been implicated in various diseases, including cancer (Pillai et al., 2022).

In physiological conditions KEAP1 is a cytoplasmic protein that acts as a substrate adaptor for Cullin 3-based ubiquitin E3 ligase complex and binds to NRF2 (Fig. 7). KEAP1 directly binds NRF2 within the N-terminal of NRF2 and targets it for ubiquitin-mediated degradation. NRF2 is a transcription factor that, when activated, translocates into the nucleus and homodimerizes with MAF proteins to target the antioxidant response elements (AREs) in the promoter regions of genes involved in cellular defense mechanisms. These include genes encoding antioxidant enzymes, detoxification enzymes, and proteins involved in redox regulation (Bellezza et al., 2018).

In cancer, mutations in KEAP1 or NRF2 genes can lead to the dysregulation of the axis. Mutations in KEAP1 are often associated with impaired ubiquitination and degradation of NRF2, resulting in its stabilization and nuclear translocation under non-stress conditions (Menegon et al., 2016). The constitutive activation of NRF2 in cancer cells leads to the upregulation of its target genes, promoting antioxidant response and enhancing the cellular defense against oxidative stress (Chio et al., 2016; DeNicola et al., 2011).

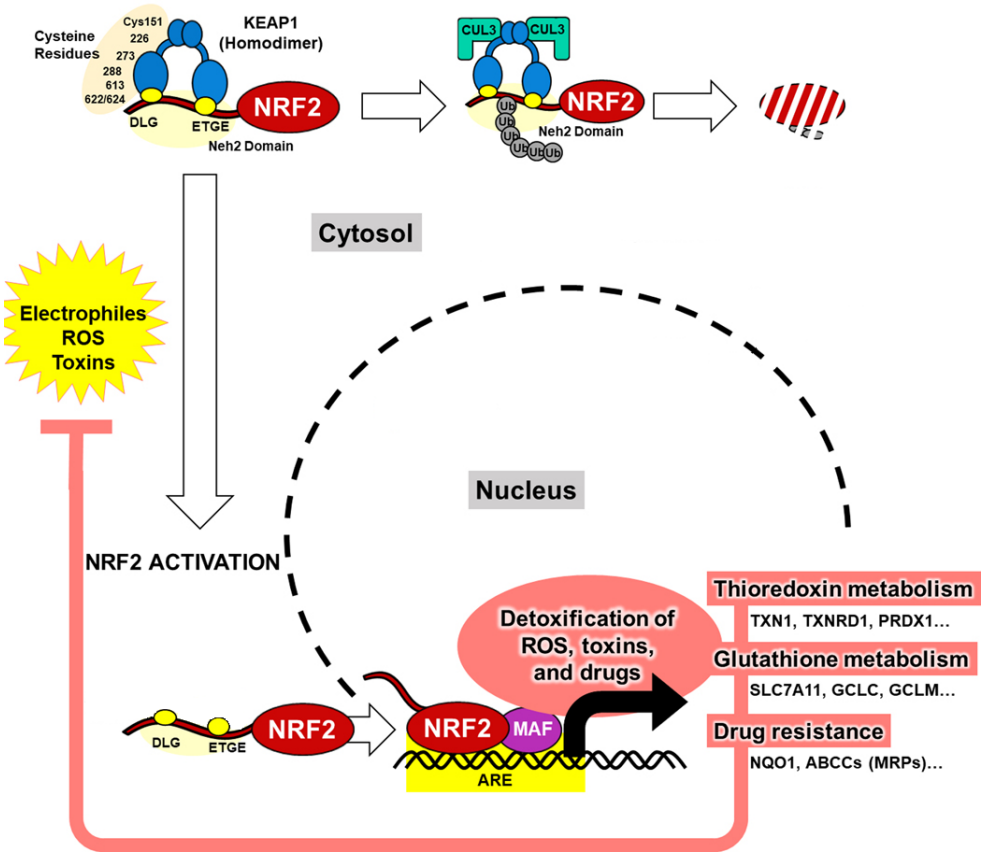

Figure 7. Schematic representation of the activation and regulation of the KEAP1-NRF2 axis. The DLG and ETGE motives essential for KEAP1-NRF2 interaction are highlighted in yellow in NRF2 representation. Adapted from Pillai et al. 2022

2 AIM

ATG5 has been extensively studied in the autophagic context however how ATG5 is involved in EMT has been poorly explored.

According to preliminary data collected in our laboratory and reported in this work, ATG5 has been found to be involved in the EMT process, as it can modulate the expression of EMT markers of TNBC cell models when it is downregulated. In contrast, overexpression of ATG5 increases the expression of mesenchymal markers. This function of ATG5 in EMT could be due to its autophagic role, but interestingly, as observed with overexpression experiments, an autophagy incompetent form of ATG5 is able to induce mesenchymal markers protein levels in a similar manner to ATG5wt. Little is known about the prognostic role of ATG5 in breast cancer patients, and how ATG5 affects EMT molecularly remains to be clarified.

On this ground, the first aim of this work is to evaluate the expression level and prognostic significance of ATG5 in breast cancer subtypes. For this purpose, we used a cohort of patients obtained from the TCGA Breast Cancer Project. In this thesis we also aim to explore the mechanism by which ATG5 is involved in the modulation of EMT by identifying with an in silico predictive analysis and an in vitro affinity purification coupled to mass spectrometry approach ATG5 non-autophagic interactors. Our data provide evidence that KEAP1 is an ATG5 interactor and this result is further confirmed by a proximity biotinylation assay used as an orthologous validation method. Finally, to explore the molecular significance of ATG5-KEAP1 interaction, we take advantage of gene set enrichment analysis of RNAseq data obtained from ATG5 downregulated models, and we assess the impact of ATG5 downregulation on the function of NRF2, a transcription factor whose protein stability depends directly on KEAP1.

3 RESULTS

3.1 PREVIOUS RESULTS: A shRNA SCREEN TO IDENTIFY NOVEL EMT MEDIATORS

The project's inception is rooted in a previously performed shRNA-based screen aimed at identify novel mediators of EMT (Fig. 8). The screen was carried out in vitro using a pooled Decipher lentiviral library (Cellecta) containing 27290 short-hairpin RNA (shRNA) sequences targeting 5000 genes.

The lentiviral library was infected in the triple negative breast cancer cell line MDA-MB-231, which exhibits EMT characteristics and low E-cadherin expression. Cells were sorted for re-expression of E-cadherin and positive hits were identified by NGS sequencing of the barcodes uniquely associated with each shRNA sequence.

The screen allowed the identification of a number of previously known EMT mediators and a number of autophagy-related genes, including SQSTM1 and ATG5. A recent paper showed that SQSTM1 contributes to EMT by degrading E-cadherin through autophagy (Damiano et al., 2020). However, the role of ATG5 in EMT was further investigated in the current work.

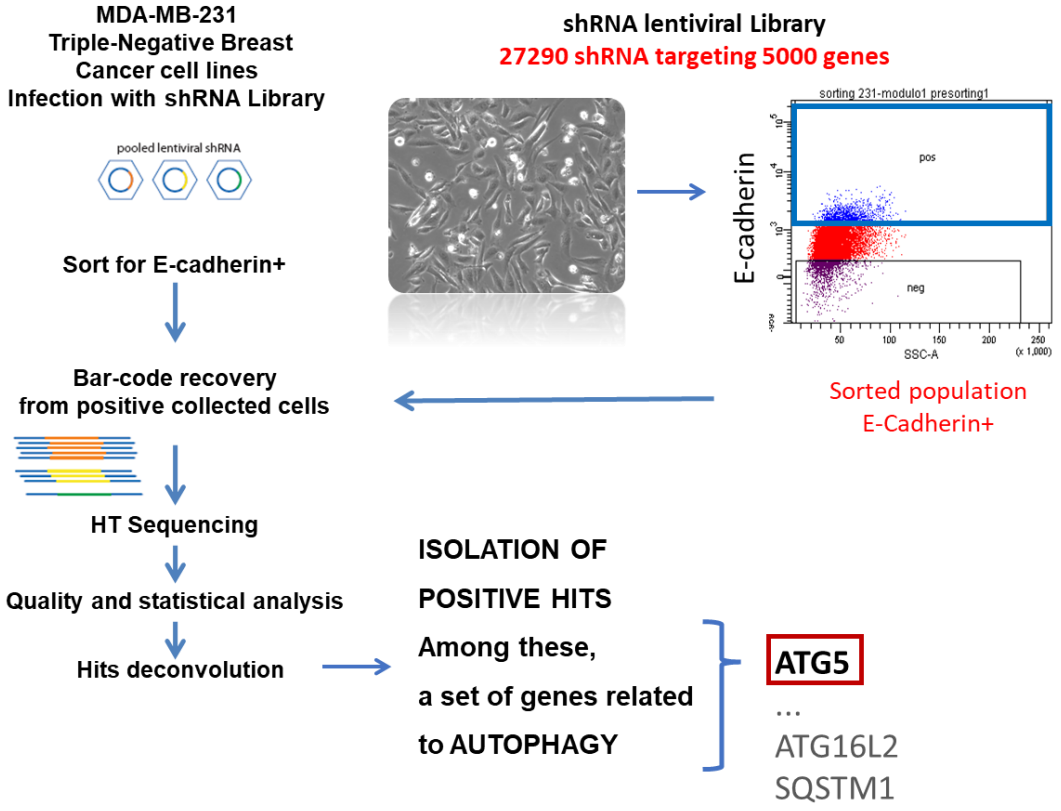

Figure 8. Workflow of the reverse-genetics screen used to identify novel mediators of EMT.

3.2 PREVIOUS RESULTS: ATG5 MODULATION AFFECTS EMT MARKERS EXPRESSION

The role of ATG5 as a possible inducer of EMT in TNBC cells was confirmed in MDA-MB-231 (the original context of the genetic screen) and in MDA-MB-157 cell lines. ATG5 was knocked down using the shRNA sequences obtained from the Cellecta library (shATG5-1, shATG5-4) (Fig. 9). Two irrelevant sequences (shGFP, shRFP) were used as negative controls. Using western blot, was verified the efficacy of ATG5 downregulation by evaluating the protein level of the ATG5-ATG12 complex. The amount of free ATG5 is undetectable under standard experimental conditions in the two cell lines. Indeed, once ATG5 is synthesized, it is covalently conjugated to ATG12 (N Mizushima et al., 1998).

ATG5 downregulation was accompanied by the accumulation of two autophagic markers, the adaptor molecule SQSTM1 and LC3-I (the non-lipidated and inactive form of LC3), which characterize autophagic block (Fig. 9A lower panels).

As expected, the ATG5 knock-down in both cell models was accompanied by an increase in the levels of the epithelial marker E-cadherin and a decrease in the levels of the major EMT-TF (ZEB1) expressed by these cells, indicating reversion of the EMT phenotype (Fig. 9A upper panels).

Since ATG5 downregulation in TNBC cell lines is associated with an attenuation of the mesenchymal phenotype, we wanted to complement these data and test whether overexpression of ATG5 can promote EMT. To this end, we overexpressed ATG5 in MDA-MB-231, MDA-MB-157 breast cancer cell lines. We used a vector expressing wild-type ATG5 (ATG5wt) and a vector expressing an autophagy-defective form of ATG5 (ATG5φdef) that carries a mutation (K130R) which prevents covalent binding between ATG5 and ATG12 (N Mizushima et al., 1998; Otomo et al., 2013).

The ectopic overexpression of ATG5wt resulted in an increase in both the ATG5-ATG12 covalent complex (56 kDa) and the amount of free ATG5. In contrast, overexpression of ATG5φdef allele, which is unable to bind ATG12, led to an increase in free ATG5 alone (35 kDa) and a slight reduction of the ATG5-ATG12 complex levels (Fig. 9B). Overexpression of ATG5wt caused an increase of the levels of the autophagic markers SQSTM1, LC3-I/LC3-II. Therefore, ATG5wt overexpression caused an increase in autophagic flux. On the other side, overexpression of ATG5φdef caused a reduction in the autophagic flux hallmarked by SQSTM1 and LC3-I accumulation in the MDA-MB-157 and an accumulation of LC3-I in

MDA-MB-231 (Fig. 9B lower panels). This effect was expected since ATG5φdef acts as a dominant negative impairing autophagy progression (Hamacher-Brady et al., 2007).

Analysis of the most representative epithelial and mesenchymal markers showed that overexpression of ATG5 in TNBC cells clearly induced the expression of vimentin and the EMT-TF ZEB1 in MDA-MB-231 and MDA-MB-157 (Fig. 9B, upper panels). In addition, upregulation of SNAI1 was observed in MDA-MB-157. SNAI1 levels in MDA-MB-231 were undetectable, as these cells do not express SNAI1. It should be noted that TNBC cell lines express low levels of E-cadherin and therefore it was not possible to evaluate a visible effect of ATG5 on this marker.

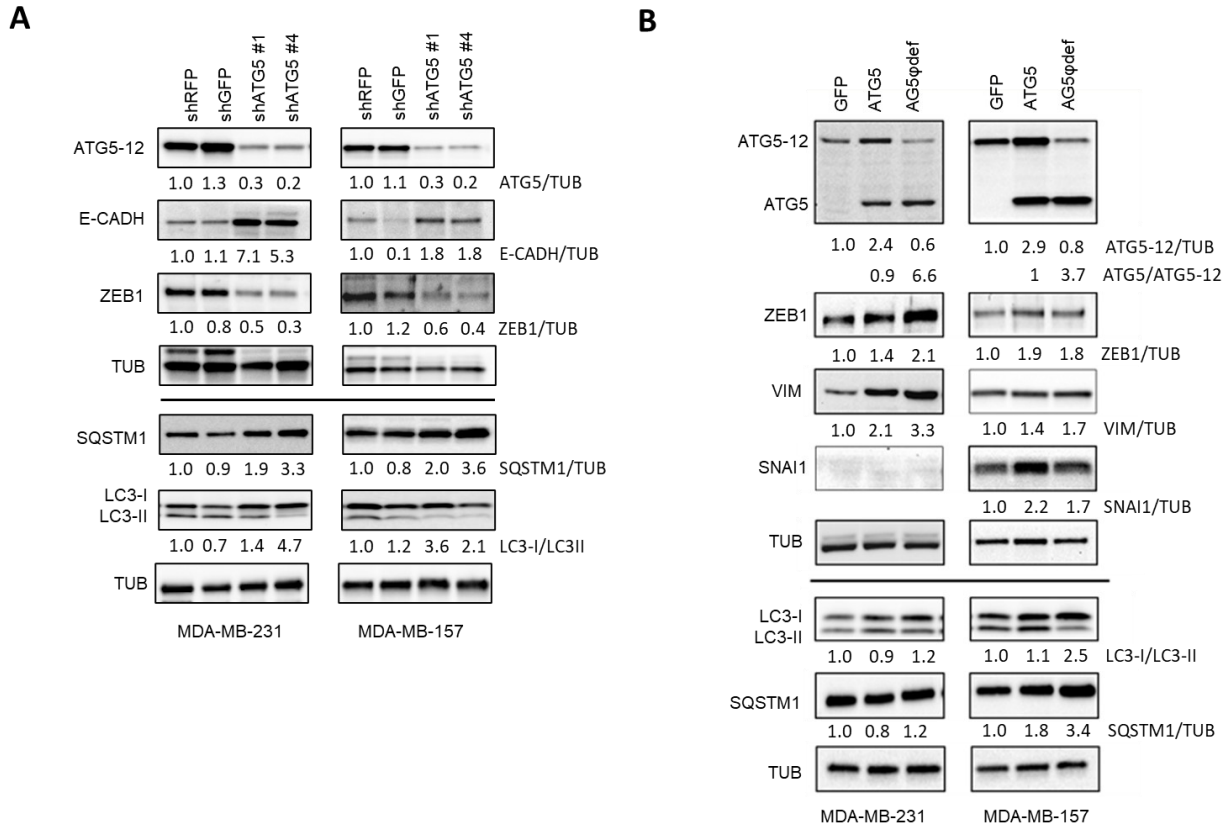

Figure 9. EMT markers are modulated upon either ATG5 knock-down or overexpression. (A) Upper panels report the expression of ATG5-ATG12, E-cadherin and ZEB1 in MDA-MB-231 and MDA-MB-157 cell models knock-down for ATG5 (shATG5#1, shATG5#4) compared to control (shRFP, shGFP). Lower panels show LC3-I/LC3-II and SQSTM1 protein levels reported as hallmarks of autophagy. Tubulin was used as a loading control. (B) Western blot analysis in cells overexpressing ATG5wt, ATG5φdef or GFP (used as control). The upper panel shows the expression of ZEB1, vimentin and SNAI1 in MDA-MB-231 and MDA-MB-157. Lower panels show LC3-I/LC3-II and SQSTM1 protein levels used as hallmarks of autophagy progression. Tubulin was used as a loading control.

These results suggest that ATG5 was able to modulate EMT in cell models with a plastic phenotype. Of particular significance, the autophagy-deficient mutant ATG5φdef modulated EMT markers in a manner consistent with the ATG5wt form. This suggests that the ability of ATG5 to modulate EMT is independent of activation of the autophagy pathway.

3.3 PREVIOUS RESULTS: ATG5 MODULATION REGULATES E-CADHERIN EXPRESSION AT TRANSCRIPTIONAL LEVEL

To further investigate how ATG5 regulates the expression of the epithelial marker E-cadherin its expression level was explored by qPCR. Downregulating ATG5 in the MDA-MB-231 and MDA-MB-157 cell models, we observed an increase in CDH1 transcript level by qPCR. This result suggests that E-cadherin regulation occurs at transcriptional level. (Fig. 10)

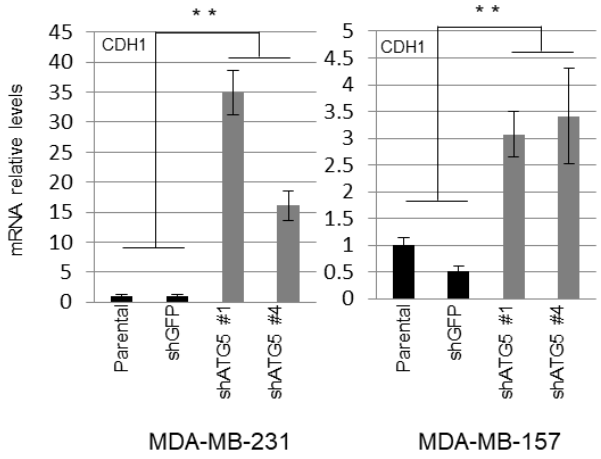

*Figure 10. ATG5 modulation controls E-cadherin at transcriptional level. Expression of CDH1 was explored by qPCR in MDA-MB-231 and MDA-MB-157ATG5 knock-down cells (shATG5#1, shATG5#4) compared to controls (parental, shGFP). Bars represent standard deviation **p-value<0.001; *p-value<0.05, Student t test.*

3.4 ATG5 EXPRESSION IS ENRICHED IN BREAST CANCER MOLECULAR SUBGROUPS SHOWING MESENCHYMAL TRAITS

According to the preliminary data, ATG5 plays a role in modulating EMT markers in vitro. To investigate whether the role of ATG5 in the regulation of EMT markers has clinical relevance, we analyzed the expression levels of ATG5 and its binding partners ATG12 and ATG16L1 in a series of breast cancer patients. For this purpose, we used patients samples expression data obtained from the TCGA breast cancer cohort of Xena Browswer (https://xenabrowser.net). We included in our analysis those tumor samples reported in (Cancer Genome Atlas Network, 2012) carrying information about overall survival and the PAM50 classification. We excluded those samples identified as normal-like subtype. The final chort was composed of 514 cases. According to the PAM50 breast cancer classification, patient primary tumor samples were assigned to the molecular subtypes Luminal A (n=231), Luminal B (n=127), HER2+ (n=58) and Basal (n=98). As expected, the majority of patients were classified as Luminal A and Luminal B, two subtypes that are know to complessively represent the 70% of all breast cancer. The higher ATG5 expression was observed in the HER2+ and Basal subgroups compared to Luminal A and Luminal B. Interestingly, in the same cohort, ATG12 and ATG16L1 levels were reduced in the Basal subgroup compared to Luminal A, Luminal B and HER2+ (Fig. 11).

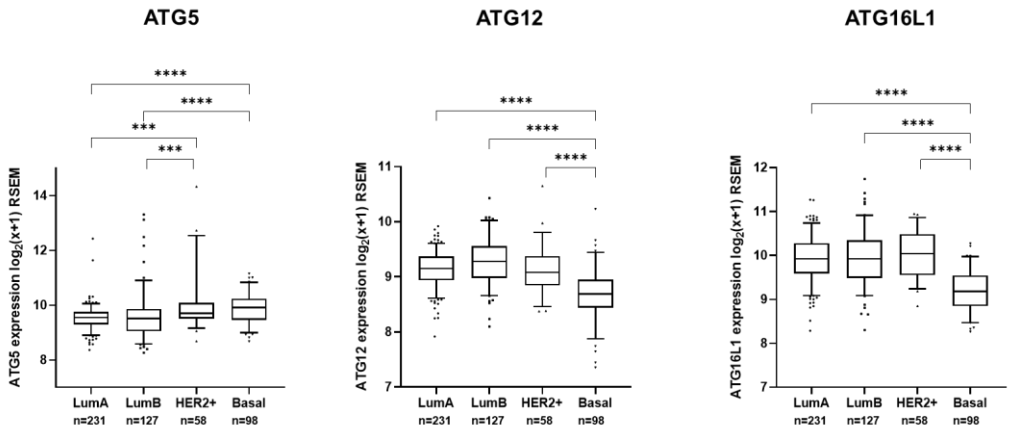

*Figure 11. ATG5, ATG12 and ATG16L1 transcript levels according to the molecular groups of TCGA BRCA cohort. The mRNA expression of ATG5, ATG12 and ATG16L1 were obtained from UCSC Xena Browser and are reported as $log_2(x+1)$ RSEM and are associated with the molecular breast cancer subgroups according to PAM50 classification obtained from UCSC Xena Browser. In the boxplots the upper and lower edges of the rectangles represent the 75th percentile and the 25th percentile respectively. The line within the rectangles shows the median value of expression (50th percentile). The whiskers show the 95th and 5th percentiles. Individual dots indicate outliers. ***p-value<0.001; ****pvalue<0.0001, Kruskal-Wallis Test.*

3.5 BREAST CANCER PATIENTS OVERALL SURVIVAL ACCORDING TO ATG5 EXPRESSION

Since ATG5 expression varies in different breast cancer subgroups, we further investigated the overall survival (OS) of TCGA breast cancer patients using a Kaplan-Meier survival analysis. The entire TCGA breast cancer patient cohort (ALL BC) was divided into two groups based on the auto-cutoff option offered by KM-Plotter as ATG5 high ≥ 9.76 and ATG5 low < 9.76. Cosidering the OS of the entire cohort (Fig. 12A), ATG5-high patients showed a poor prognosis compared to ATG5-low patients. Patient survival was then evaluated within each molecular subgroup. Interestingly, Luminal B patients with high ATG5 expression (n=38) had a significantly shorter OS than patients with low ATG5 expression (n= 89) (Fig. 14C). For patients belonging to the luminal A, HER2+, and basal subgroups, there were no differences in OS based on ATG5 high and ATG5 low expression levels (Fig. 12 B, D, E). Overall, the OS analysis reported here suggests that ATG5-high expression identifies a luminal B subgroup with worst prognosis.

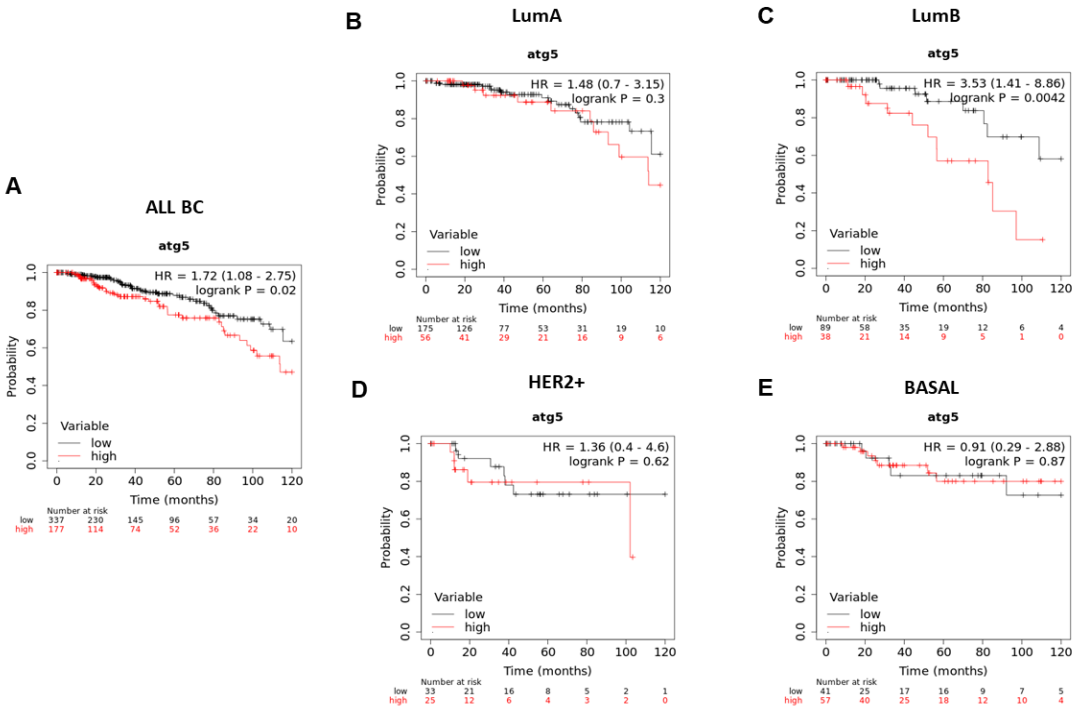

Figure 12 (A, B, C, D, E). Prognostic value of the TCGA-BRCA patients according to ATG5 expression level. Kaplan-Meier survival analysis performed using the Overall Survival data plotted with KM Plotter online tool. (A) The complete TCGA BRCA cohort was split in ATG5 high and ATG5 low according to the auto select best cutoff option. The obtained cutoff value (9.76) was further used for the other BC subgroups. (B, C, D, E) OS of ATG5 high and ATG5 low patients according to the PAM50 molecular groups of TCGA BRCA cohort.

3.6 AN AFFINITY PURIFICATION-BASED INTERACTOMIC ANALYSIS IDENTIFIES KEAP1 AS A NOVEL ATG5 INTERACTOR

The preliminary results suggest that ATG5 is able to regulate EMT markers at protein level and E-Cadherin also at transcriptional level. Curiously, ATG5 carries nuclear export and import sequences and it has been identified in previous works in cellular nuclei (Lin et al., 2020; Maskey et al., 2013), but it lacks domains able to recognize DNA. Based on this knowledge, we hypothesized that ATG5 may act in conjunction with other proteins in the modulation of EMT. To explore this possibility, we set up an interactomic analysis based on a Liquid Chromatography coupled to Mass Spectrometry (LC-MS/MS) approach.

MDA-MB-231 in vitro models were infected to overexpress STREP-tagged forms of ATG5φdef (STREP-ATG5φdef) and a control STREP-empty vector. The overexpressed molecules found in cell protein lysates were then pulled-down using a resin specifically interacting with the STREP tag.

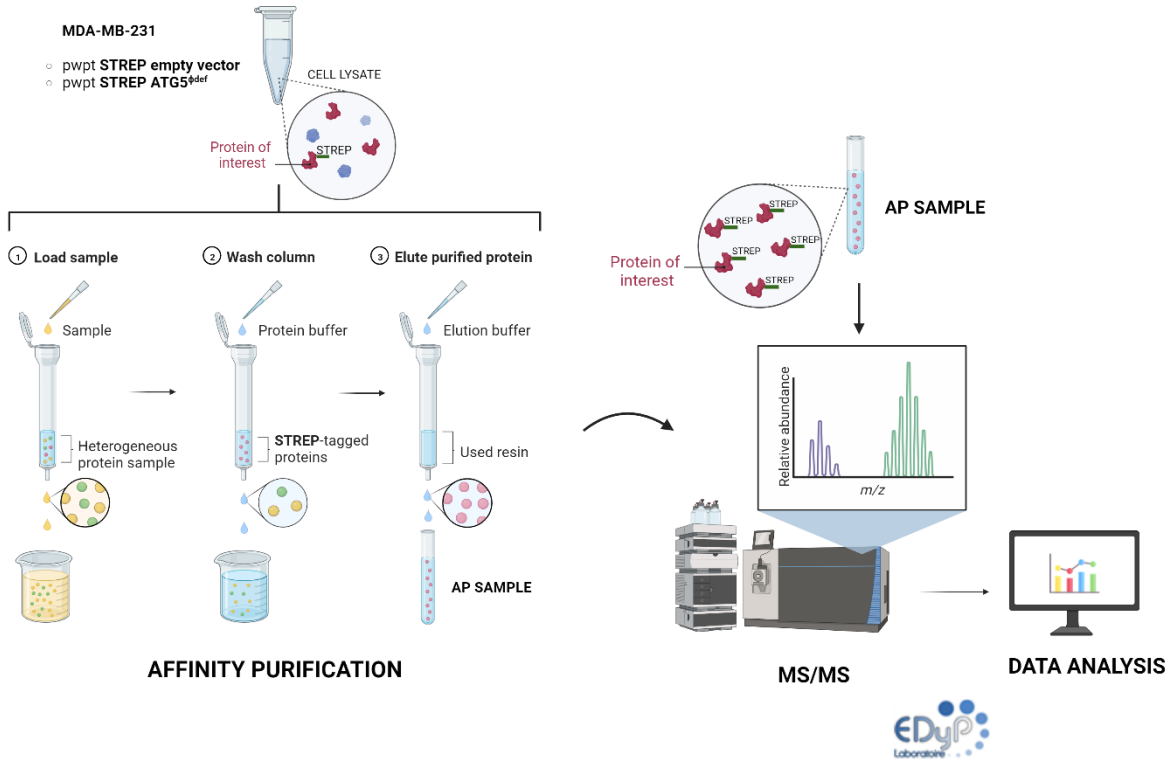

Figure 13. Schematic representation of the Affinity purification coupled to LC-MS/MS experimental approach.

The proteins isolated together with STREP-ATG5φdef were then identified and quantified by LC-MS/MS in collaboration with EDyP Laboratory (Institut de Recherche Interdisciplinaire de Grenoble – Grenoble) (Fig.13). The ATG5φdef binding partners were filtered considering a $Log_2FC > 0.6$ and a $p < 0.05$. The nonspecific interactors were excluded based on the STREP-empty samples interactome. Furthermore, 6 proteins (SQSTM1, ATG12, ATG16L1, ATG16L2, ATG5) known for their involvement in the autophagic pathway, were excluded from ATG5φdef interactome. In the end we obtained 26 putative ATG5φdef interactors (Table 1).
It should be noted, that ATG5φdef is still able to homodimerize with ATG5wt and partially allow ATG5-ATG12-ATG16L1 complex formation.

ATG5ϕdef vs CTRL			
	GENE NAME	**log_2 FC**	**p-value**
1	DCAF4L1	6.04	9.55E-12
2	CAMSAP3	4.39	1.15E-08
3	PSMD6	2.75	1.37E-05
4	CCT5	3.24	2.44E-05
5	CCT4	3.91	8.57E-05
6	TCP1	3.42	1.45E-04
7	CCT6A	3.87	2.33E-04
8	OGT	2.56	3.88E-03
9	AXL	1.70	4.05E-03
10	CCT3	2.14	4.08E-03
11	CCT8	2.94	4.37E-03
12	CCT2	2.76	4.57E-03
13	CCT7	3.38	5.13E-03
14	MATR3	2.53	1.80E-02
15	HMGB1	1.29	1.92E-02
16	COL13A1	1.32	1.96E-02
17	KEAP1	1.07	2.52E-02
18	DDX3X	1.93	2.83E-02
19	RELA	0.78	3.42E-02
20	XRN2	1.10	3.57E-02
21	CDC73	1.55	4.39E-02
22	THBS1	1.62	4.53E-02
23	ERLIN1	0.85	4.55E-02
24	ZC3HAV1	1.20	4.70E-02
25	SLC25A3	0.97	4.83E-02
26	DNAJA1	0.83	4.98E-02

Table 1. ATG5φdef interaction partners identified by LC-MS/MS of STREP-tagged constructs. The list reports the putative interaction partners for ATG5φdef compared to control EMPTY vector. The reported genes were filtered from the LC-MS/MS interaction list using

Beyond the autophagy related proteins identified as ATG5 interaction partners, a number of non-autophagic ATG5φdef interactors was identified. According to a Metascape analysis (Fig. 14) some of those proteins have chaperonic roles, a number of proteins is involved in immune related processes as: apoptotic cell clearance, innate immune response and neutrophil degranulation. Finally, some ATG5 interactors are involved in proteasomal degradation. Interestingly, among them, we identified KEAP1 as an ATG5φdef interactor. This protein is involved in ubiquitin mediated proteolysis and in pathways for the regulation of NRF2 transcription factor.

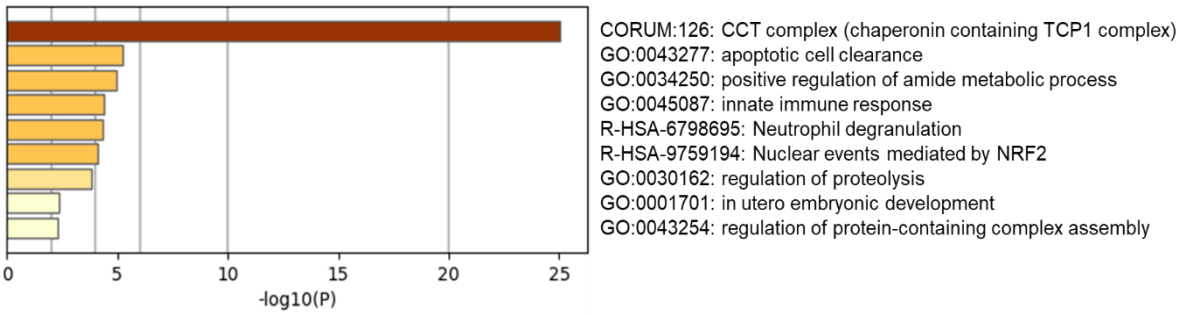

Figure 14. Metascape analysis for the non-autophagic ATG5 interaction partners identified by affinity purification coupled to LC-MS/MS approach.

3.7 KEAP1 IS AN ATG5 INTERACTOR PREDICTED BY THE HUMAN INTEGRATED PROTEIN-PROTEIN INTERACTION REFERENCE TOOL

To further acquire information about the putative interaction between ATG5 and KEAP1 we queried the Human Integrated Protein-Protein Interaction rEference (HIPPIE) database. HIPPIE is a web tool collecting experimentally measured human protein-protein interactions (PPI) from several publicly available datasets (BioGRID, DIP, HPRD, IntAct, MINT, BIND, and MIPS) (Alanis-Lobato et al., 2017).

Using this tool, it was possible to look for ATG5 interactors reported in literature. ATG5 partners are scored based on the type of the interaction (a value defined by HIPPIE to numerically express the reliability of the evidence supporting the interaction). We selected all the putative interaction partners (physical association, direct interacton or association) with a score higher than 0.7 (Fig 15A).

Only proteins recorded as direct ATG5 interactors (direct interaction is defined by Hippie as interaction between molecules within the same physical complex) were then selected. They are represented as a network in figure 15B.

A number of proteins involved in the autophagic pathway were reported as direct interactors of ATG5 (upper part of the graph), among them some known ATG5 autophagic partners (TECPR1, ATG16L1, ATG3). The lower part of the graph reports the interactors of ATG5 that were not associated to an obvious autophagic function, and among them was identified KEAP1 with a score of 0.73. The ATG5-KEAP1 interaction is supported by 2 yeast two hybrid screens (Luck et al., 2020; Rolland et al., 2014). KEAP1 was the only protein found as ATG5 interactor by our LC-MS/MS experiments supported by this tool.

A

INTERACTOR	SCORE
ATG16L1	0.97
ATG12	0.97
TECPR1	0.9
ATG16L2	0.88
ATG3	0.88
CCDC12	0.87
MAVS	0.87
RB1CC1	0.87
MAP1LC3B	0.84
SQSTM1	0.84
WIPI2	0.83
ATG10	0.79
WDFY3	0.79
OPTN	0.78
RAB33B	0.78
ATG5	0.77
BIRC5	0.75
CCHCR1	0.74
HTT	0.73
KEAP1	0.73
RAB33A	0.73
TEKT4	0.73
FAS	0.73
UCHL1	0.73
ATG13	0.72
ATG101	0.72
EXOC4	0.72
IKBIP	0.72
IMPDH2	0.72
IRGM	0.72
MAP1LC3C	0.72
SIRT1	0.72
TKT	0.72
ULK1	0.72
FADD	0.7

B

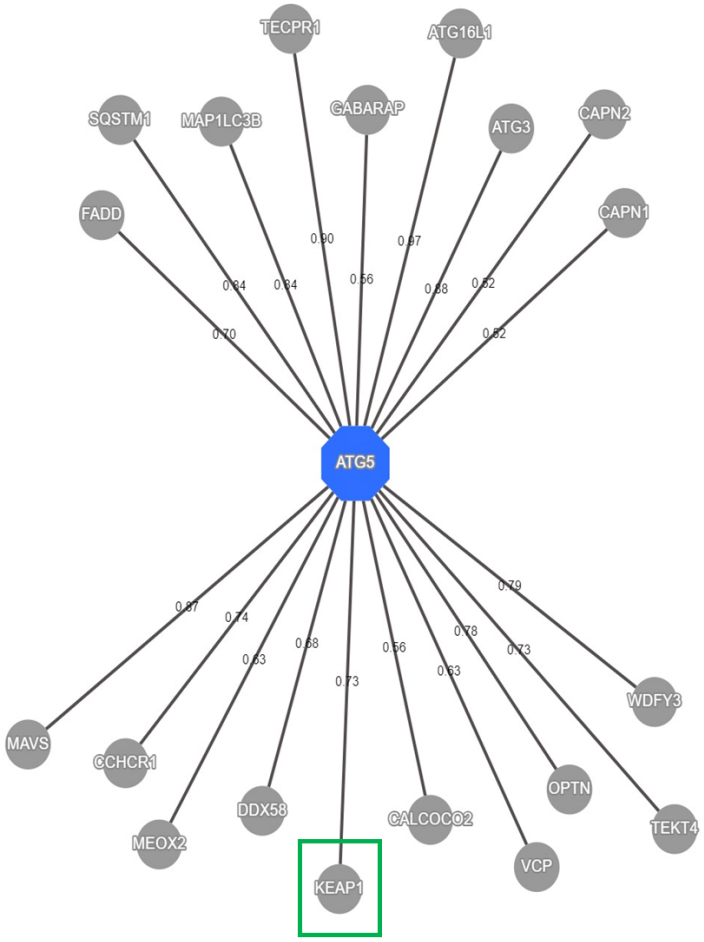

Figure 15. ATG5 interactors reported in the HIPPIE repository. (A) Table reporting the interaction partners identified as physically associated, direct interactors or associated with ATG5 with a reliability score higher than 0.7. (B) graphical representation of the direct interactors of ATG5, the upper part of the figure reports the autophagy-involved proteins, the lower part the non-autophagic ATG5 interactors. Numbers on edges represent the reliability score of interaction.

3.8 KEAP1 IS CONFIRMED TO INTERACT WITH ATG5 USING AN AFFINITY PURIFICATION APPROACH

To confirm the interaction between ATG5 and KEAP1 identified by the LC-MS/MS approach and supported by the literature reported in Hippie, an affinity purification approach analogous to the one used for the interactomic study was set up using HEK 293T cells ectopically expressing flag-KEAP1 together with strep-ATG5 or strep-ATG5φdef constructs.

Comparable expression of flag-KEAP1 and strep-tagged constructs was obtained between samples, as shown in the input (Fig. 16, left). Strep-tagged constructs were then pulled down using a streptactin resin.

As shown in Figure 16, KEAP1 was mildly but specifically identified in the ATG5-enriched lysates compared to the lysates enriched for Strep- control constructs (Strep-Empty vector used in the LC-MS/MS interactomic experiments and Strep-Renilla). KEAP1 was more enriched with the strep-ATG5φdef construct, but as indicated by the strep signal, this effect could be the result of differential efficiency in the pull-down of the strep constructs. As a positive control for pull-down, a flag-tagged form of ATG16L1 was overexpressed in combination with strep-ATG5. ATG16L1 is a known ATG5 interactor and, as expected, was successfully enriched, confirming the efficacy of the technique.

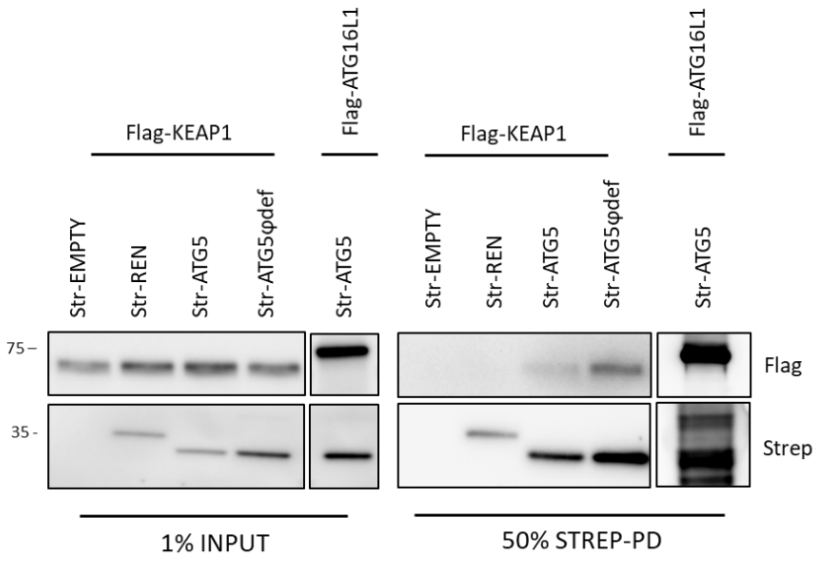

Figure 16. Binding of flag-KEAP1 to strep-ATG5 and strep-ATG5φdef. HEK 293T cells were transfected with strep-ATG5, strep-ATG5φdef and control constructs (strep-EMPTY, strep-REN), flag-KEAP or control construct (flag-ATG16L1). Cell lysates were affinity purified by strep-tag interaction with a streptactin resin, then the purified lysates were immunoblotted for flag tag to detect KEAP1 or ATG16L1 interaction. As control of successful strep enrichment, membranes were immunoblotted with α strep antibody.

These data show that flag-KEAP1 interacts with strep-ATG5 and strep-ATG5φdef and confirm the interaction suggested by an analogous affinity purification approach for the LC-MS/MS-based interactomic experiments.

3.9 ATG5 AND ENDOGENOUS KEAP1 INTERACT BASED ON A PBD ASSAY

To further sustain the interaction identified by the affinity purification approach with an orthologous technique, we set up a proximity biotinylation assay based on TurboID technology. TurboID is a proximity labeling method in which the protein of interest (POI) is fused to a bacterial-derived biotin ligase called BirA. When the fusion protein is stably expressed in a cell line, it can biotinylate the proteins in close proximity to the POI upon exogenous biotin administration in the growth medium. Subsequently, the cell lysates can be captured using a streptavidin-based affinity purification method. Flag-tagged TurboID ATG5wt (TbIDATG5) or Flag-tagged TurboIDATG5φdef (TbIDATG5φdef) fusion proteins and control constructs were overexpressed in HEK 293T cells. Cells were treated with culture medium supplemented with biotin to allow biotinylation of endogenous proteins near the bait.

The expression level of TurboID fusion proteins was detected by anti-Flag immunoblotting and then, the enzymatic activity of the baits was detected by Streptavidin-HRP hybridization. The biotinylation profile of the total cell lysates treated with biotin was comparable in the different samples, while the control total cell lysates (treated with DMSO) showed no traces of biotinylation, as expected (Fig. 17A).

The cell lysates were then affinity purified to selectively isolate the biotinylated proteins. As shown in Figure 17B, endogenous KEAP1 was identified as a target of TbIDATG5 and TbIDATG5φdef biotinylating activity. We also observed the enrichment of p53 upon expression of the TbIDTwist1 construct, this interaction was considered as a positive control for the technique, as p53 is a known interactor of Twist1 (Piccinin et al., 2012). GAPDH, as expected, was not enriched as an interactor. These data demonstrate that ATG5 can interact with endogenous KEAP1.

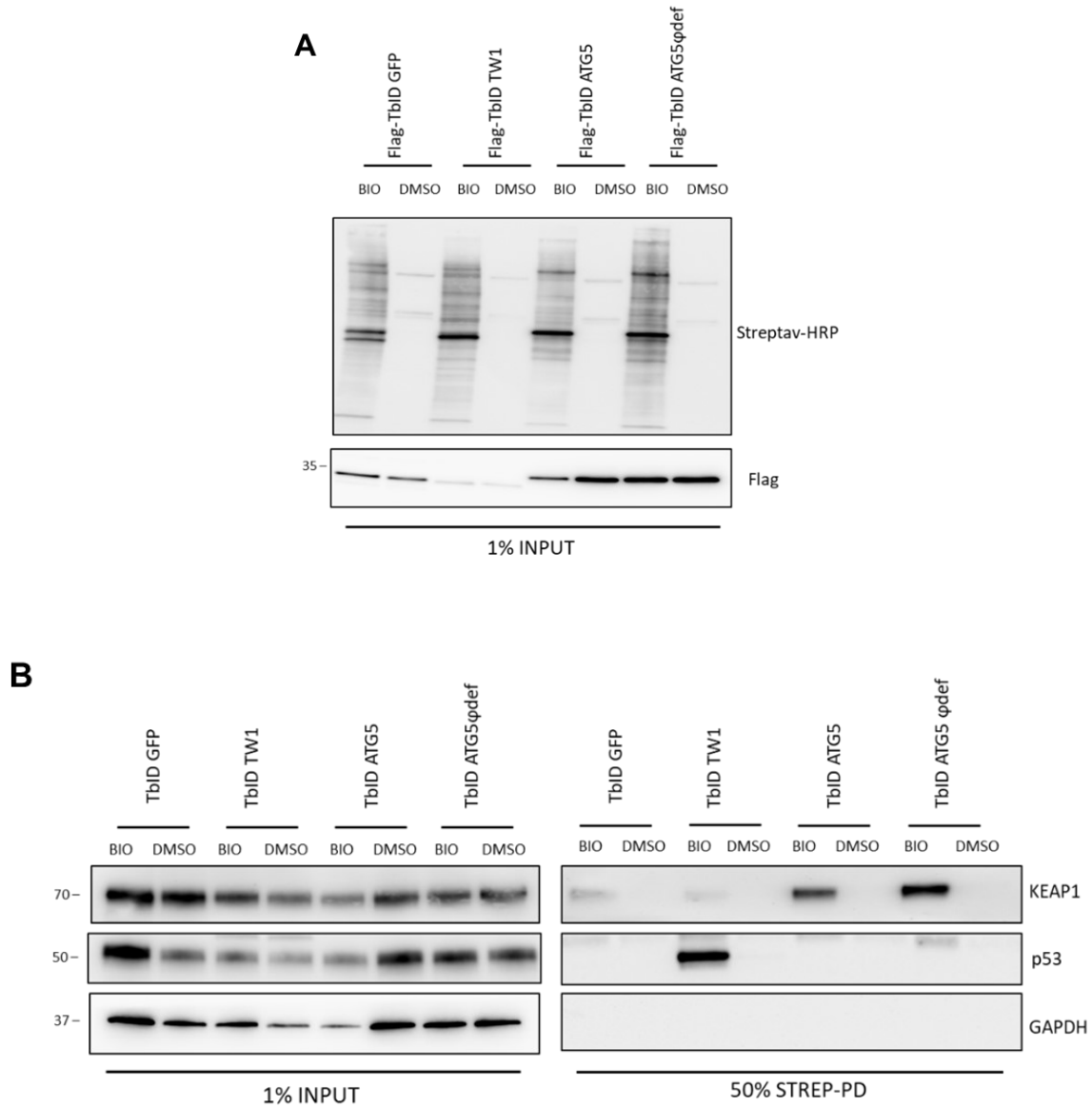

Figure 17. TurboID PBD Assay for ATG5 and KEAP1 interaction. (A) HEK 293T cells overexpressing flag TbIDATG5 and flag TbIDATG5φdef and control constructs (flag TbID GFP, flag TbID TW1) immunoblotted for flag and Streptavidin-HRP. (B) Immunoblot analysis of eluates obtained by strep-tactin based enrichment of biotinylated proteins. 1% input lysate is reported as reference for protein abundance before strep-tactin enrichment. To evaluate the interaction input and eluates were immunoblotted for KEAP1, p53, and GAPDH.

3.10 MODULATION OF ATG5 IN TNBC CELLS AFFECTS NRF2 EXPRESSION AND TARGET GENES

After having identified and validated the interaction between ATG5 and KEAP1, we investigated whether this interaction has an effect on the KEAP1/NRF2 axis. First, we examined the protein expression of NRF2 and KEAP1 in MDA-MB-231 cells in which ATG5 was knocked down. Downregulation of ATG5 (Fig. 18A) leads to an increase in NRF2 protein levels, whereas KEAP1 protein levels are slightly increased in an ATG5 downregulated context suggesting that ATG5 has probably no role in KEAP1 modulation but it might act in conjunction with KEAP1 to control NRF2 levels.

To further investigate the effect of NRF2 increase upon ATG5 downregulation in our model, we utilized an RNAseq analysis previously performed in our laboratory on MDA-MB-231 ATG5 knockdown cells and performed a Gene Set Enrichment Analysis (GSEA). A NRF2 target genes signature (NAMANI_BOCCI_NRF2_UP) was built from a literature based on (Bocci et al., 2019; Namani et al., 2017), moreover a signature (SINGH_NRF2_UP) based on (Singh et al., 2021) was obtained from the Broad Institute Molecular Signatures Database. As shown in Figure 18B, a significant enrichment of genes was found in the MDA-MB-231 ATG5 knockdown samples.

This result suggests that the increased NRF2 protein level is associated with upregulation of NRF2 target genes in ATG5 knockdown. Overall, these results suggest that downregulation of ATG5 leads to increased expression of NRF2 target genes.

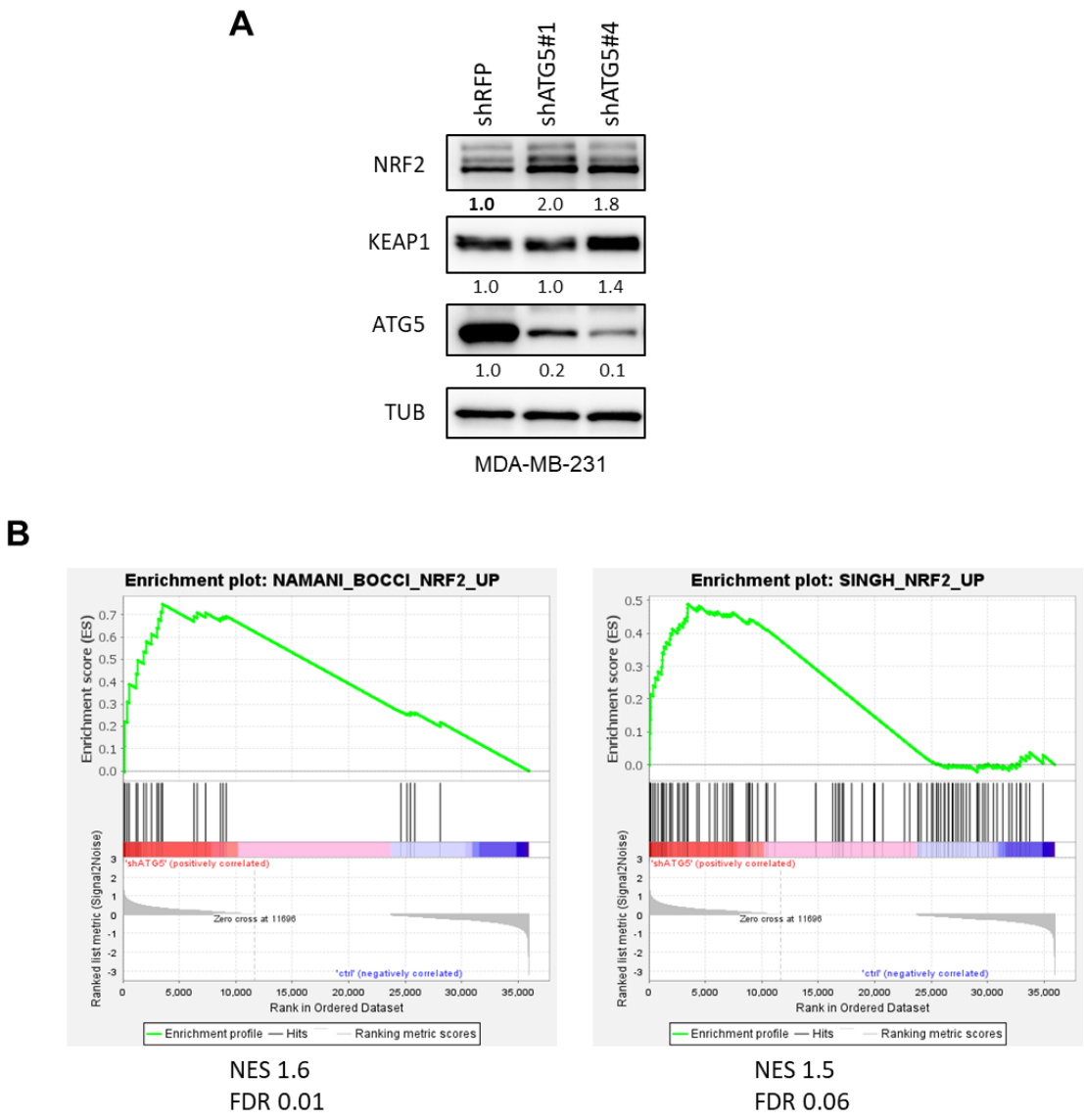

Figure 18. ATG5 downregulation affects NRF2 protein levels and NRF2 target genes expression. (A) Western Blot for the expression of NRF2, KEAP1 and ATG5 in MDA-MB-231 shATG5 (shATG5#1, shATG5#4) compared to control (shRFP). Tubulin was used as loading control. (B) GSEA enrichment results for two signatures for NRF2 downstream targets. The plots show an enrichment of both signatures in MDA-MB-231 shATG5 class. The Y axis reports the enrichment score (ES), the X axis shows the gene enrichment between shATG5 (left) and control (right). In the figure NES (normalized enrichment score) and FDR (false discovery rate) are reported.

4 DISCUSSION

In this study, we describe an unconventional role of ATG5, one of the key molecules of autophagy, as an inducer of the EMT phenotype. ATG5 emerged from a phenotypic screen aimed at identifying modulators of EMT in breast cancer cells. The role of ATG5 was confirmed using in vitro genetic manipulations demonstrating that ATG5 sustains the mesenchymal properties of TNBC cells. Moreover, ATG5 was found to modulate the EMT phenotype independently of the interaction with its canonical autophagic partner ATG12, thus suggesting a novel function for ATG5 in regulating the EMT phenotype.

We therefore studied the overall survival of breast cancer patients and the expression levels of ATG5 and its autophagic binding partners ATG12 and ATG16L1. The study of overall survival in a series of primary breast tumors showed that ATG5 plays a prognostic role for the Luminal B patients. The luminal B subgroup includes tumors with a more aggressive behavior and a worse prognosis compared to Luminal A group. In addition, luminal B cancers show increased recurrence rates in the first 5 years after diagnosis and a similar time pattern of metastatic dissemination as basal-like and HER2-enriched cancers (Ades et al., 2014). Characterization of peculiar molecular alterations is leading to the identification of agents that define more precisely luminal tumors behavior. In this context, ATG5 expression seems to be useful to identify and stratify patients with the worst prognosis among luminal B subtype.

Evaluation of ATG5 levels the same patients cohort used for the survival analysis revealed that ATG5 transcript expression is particularly high in the breast cancer basal subgroup. On the other hand, ATG16L1 and ATG12 are downregulated in the basal subgroup, suggesting a possible non-autophagic function of ATG5. The existence of autophagy-independent functions for proteins belonging to the autophagic machinery is an emerging topic (Galluzzi & Green, 2019; H. Guo et al., 2018). For example, a non-canonical function has been proposed for LC3, which appears to promote anoikis in ovarian cancer cell models with a mechanism independent of autophagy (Satyavarapu et al., 2018). Similarly, a role for FIP200 in the maintenance and differentiation of neural stem cells independent of the autophagic process has been proposed (Liu et al., 2021). Functions that are not subordinate to the autophagic process have also recently been discovered for ATG5. In particular, ATG5 has been shown to interact with molecules with E3 ubiquitin ligase activity and form macromolecular complexes with functions independent of the canonical partner ATG12. In a paper by Li and collaborators ATG5 was found to bind the ubiquitin ligase FBXW7 and form a complex that promotes proteasomal degradation of the c-MYC oncogene (S. Li et al., 2021).

A LC-MS/MS-based interactomic analysis coupled to the interrogation of the interactomic database Hippie (Luck et al., 2020; Rolland et al., 2014) allowed us to identify another ubiquitin ligase, KEAP1, as an ATG5 interactor. The interaction was confirmed by two orthologous techniques: affinity purification and the TurboID proximity biotynilation assay. It would be useful to further confirm the interaction between ATG5 and KEAP1 in endogenous conditions by immunoprecipitation exploiting MDA-MB-231, as this cell line represents the background of our study.

We investigated whether ATG5 can affect protein levels of NRF2, the major transcription factor negatively regulated by KEAP1. Indeed, we observed that downregulation of ATG5 caused an increase in NRF2 levels and upregulation of canonical NRF2 target genes. Whether NRF2 has an EMT-promoting or EMT-restraining function is currently controversial, and recent reports suggest that this relationship probably is context-dependent and may vary between different cancer types and stages (Rojo de la Vega et al., 2018). NRF2 has been shown to influence the expression of genes that are important regulators of EMT. For example, activation of NRF2 has been associated with downregulation of the EMT-promoting transcription factor SNAI1 (W. Zhou et al., 2016) and the activation of NRF2 downstream targes HMOX1 and NQO1 reduces Numb-mediated EMT (Zhang et al., 2018). On the other hand, HMOX1 accumulation induced by NRF2 activation can cause stabilization of mesenchymal transcription factor BACH1 and contribute to the poor prognosis in lung cancer patients (Lignitto et al., 2019). NRF2 is able to transcriptionally repress E-cadherin by binding its promoter region (Arfmann-Knübel et al., 2015) and it can promote migration and invasion by modulating the RhoA-ROCK1 pathway (Ko et al., 2021). According to these studies, NRF2 can either play a role in reducing EMT or promoting it.

The controversial function of NRF2 in EMT has led to the discussion of a possible NRF2 role as a phenotypic stability factor of partial EMT (Bocci et al., 2019; Vilchez Mercedes et al., 2022). Partial EMT has been defined as a mixed epithelial/mesenchymal phenotype that has been associated with a greater proliferative capacity of cancer cells compared to fully mesenchymal cells (Brabletz et al., 2021; Gupta et al., 2019). Moreover, cells with partial EMT have the ability to disseminate as clusters rather than single cells and survive to a greater extent in the bloodstream (Pastushenko et al., 2018). Studies have shown that breast cancer cell populations comprise cells that have both epithelial and mesenchymal markers, conferring them greater aggressiveness (Grosse-Wilde et al., 2015; Kröger et al., 2019). In basal breast cancer, cells located at the migration front (leader cells) exhibit high mobility and co-express epithelial

and mesenchymal markers (Dang et al., 2015). In luminal breast cancer, the leader cells show molecular signatures of partial EMT and the context of collective invasion, these cells show high plasticity to maximize their invasive capacity (C. Yang et al., 2019). Whether partial EMT is occurring in our experimental models cannot be determined based on the data here reported. To confirm ATG5-KEAP1-NRF2 circuit, KEAP1 and NRF2 should be modulated (overexpressed or downregulated) in combination with ATG5 to assess the effect on NRF2 downstream targets. Moreover, the phenotype of these models should be evaluated (EMT markers expression, cellular invasion capability). It also remains to be clarified how ATG5 controls E-cadherin expression considering a possible regulation of ATG5 on NRF2 activity. Moreover, it remains unknown how ATG5-KEAP1 interaction regulates NRF2 protein levels. The most obvious possibility is that ATG5 could interact with KEAP1 to boost NRF2 proteasomal degradation.

Importantly, it should be considered that KEAP1 is an autophagic substrate of SQSTM1. In a study by Komatsu et al. it was found that the sequestration of KEAP1 by SQSTM1 in a state of autophagic block enables the stabilization of NRF2 (Komatsu et al., 2010). The possible influence of the autophagic block in NRF2 activation was not investigated in the current study. KEAP1 has a number of functions beyond NRF2 regulation in cellular homeostasis in which ATG5 may be involved. KEAP1 has been identified in focal adhesions and adherens junctions, where it has been suggested to be responsible for maintaining the integrity of adhesion complexes during actin cytoskeletal reorganization events (Velichkova & Hasson, 2003, 2005). However, these proposed functions of KEAP1 have not been deepened in further studies. In summary, the details of the molecular mechanism regulating the ATG5/KEAP1/NRF2 axis have not been fully revealed in this work and further efforts are needed to clarify how ATG5-KEAP1 interaction influences the mesenchymal features of breast cancer.

5 CONCLUSIONS AND FUTURE PERSPECTIVES

Overall, we found in this study that high ATG5 expression is associated with a poorer prognosis in luminal B breast cancer subtype. We examined the ATG5 interactome to identify other proteins that may be involved with ATG5 in EMT regulation and identified KEAP1 as an ATG5 interactor. Finally, we provide preliminary results suggesting a role of ATG5-KEAP1 interaction in the regulation of NRF2 controlled transcription.

Further studies are required to rule out the contribution of SQSTM1 to the ATG5-KEAP1-NRF2 axis. Moreover, NRF2 protein availability is known to be regulated by KEAP1. Therefore, assessment of NRF2 protein stability upon ATG5 modulation could be useful to verify the effect of the KEAP1-ATG5 axis. In addition, identification of NRF2 targets that are upregulated upon ATG5 downregulation would help to elucidate the role of the ATG5-KEAP1-NRF2 axis

In particular, understanding the molecular consequences of the ATG5-KEAP1-NRF2 interaction will clarify how this axis is involved in EMT or partial EMT in a context-dependent way.

6 MATERIALS AND METHODS

6.1 PATIENTS EXPRESSION DATA AND SURVIVAL ANALYSIS

RNA-seq data for ATG5, ATG12, ATG16L1 and patients clinical data (PAM50 mRNA, OS event, OS time) according to (Cancer Genome Atlas Network, 2012) of the Breast Cancer TCGA cohort (TCGA BRCA) were obtained from UCSC Xena Browser (https://xenabrowser.net). Expression levels of ATG5, ATG12 and ATG16L1 were divided based on the PAM50 mRNA classification and samples were filtered to select Luminal A, Luminal B, HER2+ and Basal subgroups and it were excluded Normal Like subgroup, normal samples, and unclassified samples.

Survival analysis was performed using the online app Kaplan Meier-Plotter (https://kmplot.com/analysis/) for custom data uploading a .csv file pepared based on the data obtained from the UCSC Xena Browser and formatted as required by the system (PatientID, Survival time, Survival event, gene symbol - ATG5). The cutoff threshold was set as auto best cutoff for the "ALL BC" analysis then, the 9.76 value was used for the evaluation of all the BC subgroups. No filter option was selected and plot options were kept as default.

6.2 CELL LINES

The triple-negative human breast cancer cell lines MDA-MB-231, MDA-MB-157 and the human embryonic kidney line HEK 293T were obtained from ATCC (American Type Culture Collection, Manassas, VA, USA). HEK 293T cells, expressing the SV40T antigen, are used as a packaging line for the production of lentiviral vectors and for transfections. The cell lines were maintained in culture at 37°C in a humidified atmosphere with 5% CO2. MDA-MB-231, MDA-MB-157 cell lines were grown in MEM medium (Minimum Essential Medium, Gibco) supplemented with 10% fetal bovine serum (FBS, Gibco), non-essential amino acids (NEAA) and gentamicin 10 µg/ml (Fisiopharma). The HEK 293T cell lines were cultured in DMEM (Dulbecco's Modified Eagle's Medium, Gibco) supplemented with 10% FBS and gentamicin 10 µg/ml (Fisiopharma). Cell lines are periodically authenticated by short-tandem repeat profiling and assessed for the presence of mycoplasmas by PCR.

To generate ATG5-silenced or stably overexpressing cell models, MDA-MB-231 cells were infected using lentiviral supernatants. The lentiviral supernatants were obtained by co-transfecting, via the calcium phosphate method, HEK 293T cells with the vectors either for gene silencing (pRSI9) or for ectopic expression (pWPT) together with the lentiviral packaging

vectors (psPAX2 and PMD2.G). In detail, HEK 293T cells were seeded in 6-well plates to obtain, at the time of transfection (24 hours later), a confluence of 50-60%. At the time of transfection, chloroquine (25 μM) was added to the culture medium in order to prevent lysosomal degradation of exogenous DNA. Then, cells were transfected with the DNA-calcium phosphate complexes prepared using 2X BBS, 2.5 M CaCl2, and 6 μg of DNA (2 μg of pRSI9 or pWPT, 2.6 μg psPAX2, and 1.4 μg PMD2.G). The culture medium into which the viral particles were released, conventionally defined as "lentiviral supernatant", was collected 48 hours after transfection.

For lentiviral infection cells to be infected were trypsinized the and resuspended in culture medium added with protamine sulphate (final concentration 4 μg/ml) before plating. Protamine sulfate is a cationic polymer that increases the efficiency of viral infection.

Cells infected with pRSI9 vectors were selected with Puromycin (1 μg/mL for MDA-MB-231 and 0.5μg/mL for MDA-MB-157) 24-48 hours after infection for 3-5 days.

MDA-MB-231 models overexpressing STREP-ATG5φdef, were generated by infection with pWPT vectors containing the STREP-ATG5φdef or control (STREP-EMPTY) coding sequences. The infection efficiency was verified by Western-Blot and immunofluorescence with anti-STREP antibodies.

HEK 293T cells were transfected with the vectors pCS3strepEMPTY, pCS3strepRENILLA, pCS3strepATG5, pCS3strepATG5φdef, pcDNA3.1flagKEAP1 or pflagCMV10-ATG16L1 for the AP Assay. DNA-calcium phosphate complexes were prepared using 2X BBS, 2.5 M CaCl2, and 5 μg of DNA (2 μg of pcs3strep vectors, 2 μg of pcDNA3.1flagKEAP1 or pflagCMV10-ATG16L1 and 1 μg Salmon Sperm DNA) for a 3.5 cm plate.

HEK 293T cells were transfected with the vectors pflagATG5TbID pflagATG5φdefTbID pflagTwist1TbID and pflagGFPTbID for the PBD Assay. DNA-calcium phosphate complexes were prepared using 2X BBS, 2.5 M CaCl2, and 7 μg of DNA (4 μg of pflagTbID vectors, 3 μg Salmon Sperm DNA) for a 10 cm plate.

6.3 VECTORS GENERATION AND SEQUENCING

In the present study, the expression vectors pCS3, pWPT, pflagTurboID, pRSI9 and the vectors encoding the proteins essential for the lentiviral packaging process psPAX2 and PMD2.G were used.

pWPTGFP was obtained by Addgene, #12255. pWPT ATG5 and pWPT ATG5φdef vectors were kindly donated by prof. Simmons (Bern).

To obtain pCS3strepATG5 and pCS3strepATG5φdef vectors ATG5, ATG5φdef were amplified by PCR from the pWPT ATG5 and pWPT ATG5φdef vectors with oligos allowing the insertion of NcoI at 5':

Fw	5'-AAAAACCATGGCCACAGATGACAAAGATGT-3'
Rev	5'-AAGCAGCGTATCCACATAGC-3'

after NcoI/XhoI digestion the sequence was cloned in the Strep-Tag Ppsg105 vector (IBA LifeSciences, #5-4105-001) to obtain STREP-tagged coding sequences. To obtain pCS3strepRENILLA the RENILLA sequence obtained from PRL-CMV-Renilla (Promega, #E2261) was digested by NcoI/XbaI and was cloned in the Strep-Tag Ppsg105 vector, then the consturcts were cloned in pCS3 vector by BamHI/XhoI digestion. pWPTstrepGFP was obtained by cloning GFP sequence obtained from pWPTGFP digested by NcoI/XbaI in the Strep-TagPpsg105 vector and then cloned in the pWPT vector by BamHI/XhoI digestion. pWPTstrepATG5, pWPTstrepATG5φdef were obtained by restriction cloning of the pCS3strepATG5 and pCS3strepATG5φdef by BamHI/SalI and inserted in the pWPT backbone obtained from pWPTGFP.

pflagATG5TbID pflagATG5φdefTbID pflagTwist1TbID and pflagGFPTbID were obtained by cloning ATG5, ATG5φdef and GFP obtained from the pWPT constructs in the flagTurboID vector (Addgene, #124646) by BamHI/XhoI digestion. TWIST1 was obtained from a construct available in our laboratory and inserted BamHI/XhoI into flagTurboID vector. All the inserts were mutagenized to remove their STOP codon and insert a XhoI restriction site to allow in-frame expression with the TurboID biotin ligase.

3xFlag-CMV10-ATG16L1 was obtained by Addgene, #24302

PcDNA3.1KEAP1flag vector was syntetized by GenScript.

The silencing of ATG5 was achieved by exploiting the RNA interference pathway mediated by short-hairpin RNAs cloned in pRSI9 (shATG5#1 and shATG5#4). Two shRNA sequences directed against irrelevant genes (RFP, Red fluorescent Protein; GFP, Green fluorescent Protein) were employed as controls.

The pRSI9 vector was used for the generation of lentiviral vectors expressing the shRNA sequences directed against ATG5. Specifically, the shRNA-F and shRNA-R oligo pairs for ATG5, reported below, were designed using the publicly accessible sequences of module I of the DECIPHER library (Cellecta) and added with restriction sequences for AgeI and EcoRI useful for cloning into the pRSI9 vector:

shATG5-1-F	5'-CCGGCCTTGGAACATCACAGTATATGTTAATATTCATAGCATGTACTGTGATGTTCCAAGGTTTTTT-3'
shATG5-1-R	5'-AATTAAAAAACCTTGGAACATCACAGTACATGCTATGAATATTAACATATACTGTGATGTTCCAAGG-3'
shATG5-4-F	5'-CCGGCCTGAACAGAATCATCTTTAAGTTAATATTCATAGCTTAAGGATGATTCTGTTCAGGTTTTTT-3'
shATG5-4-R	5'-AATTAAAAAACCTGAACAGAATCATCTTTAAGCTATGAATATTAACTTAAGGATGATTCTGTTCAGG-3'
shGFP-F	5'- CCGGGCTACCTGTTCCATGGCCAGTTAATATTCATAGCTGGCCATGGAACAGGTAGCTTTTTT -3'
shGFP-R	5'- AATTAAAAAAGCTACCTGTTCCATGGCCAGCTATGAATATTAACTGGCCATGGAACAGGTAGC -3'
shRFP-F	5'- CCGGGCTCCGTGAACGGCCACGAGTGTTAATATTCATAGCACTCGTGGCCGTTCACGGAGCTTTTTT -3'
ShRFP-R	5'- AATTAAAAAAGCTCCGTGAACGGCCACGAGTGCTATGAATATTAACACTCGTGGCCGTTCACGGAGC-3'

The F and R oligos were annealed in solution, phosphorylated using T4 Polynucleotide Kinase (Promega) and cloned into the pRSI9 vector, previously digested with the restriction enzymes AgeI and EcoRI (Biolabs) and dephosphorylated, to generate directional ends and compatible with oligos.

All vectors used in this study were amplified by transformation of ultracompetent XL-10-Gold bacteria (Agilent) and selected in LB medium (LB Broth with agar - Lennox - Agar 15 g/L; NaCl 5 g/L; Tryptone 10 g/L; Yeast Extract 5 g/L, Sigma Aldrich) containing Ampicillin at a concentration of 50 ng/L (Biopharma). After the selection and amplification of the transformed colonies in LB Broth solution (NaCl 5 g/L; Tryptone 10 g/L; Yeast Extract 5 g/L, Sigma Aldrich), the plasmid DNA was extracted following the instructions of Plasmid Plus Maxi Kit (Qiagen). The purity of the extracted DNA and its concentration were determined using the spectrophotometric reading technique (280 and 260 nm, respectively) via Nanodrop2000c (Thermo Scientific). The vector coding sequences were then verified by automated Sanger sequencing using the SeqStudio genetic analyzer (Applied Biosystems®).

6.4 AFFINITY PURIFICATION

MDA-MB-231 models overexpressing ATG5 or HEK293T cells transfected with pCS3strep vectors together with pcDNA3.1flagKEAP1 or pflagCMV10-ATG16L1 were prepared as previously described. Cells were then lysed with lysis buffer (150mM NaCl, 20mM Tris-HCl pH 7.5, 1mM EDTA, 0.5% Igepal) by incubating on ice for 40 minutes. The lysate was clarified by centrifugation at 4°C for 15 minutes at 13000rpm and a portion (1%) was analyzed by western blot. 20µL of Strep-Tactin resin were added to the remaining lysate and incubated at 4°C in rotation 1 hour. The resin was then washed 5 times with the aforementioned lysis buffer. For western blot processing the proteins were resuspended in 40 µl of 2x Laemmli buffer (0.125M Tris, 4% SDS, 10% glycerol, 10% 2-mercaptoethanol, 0.004% bromophenol blue). For LC-MS/MS processing the proteins were incubated for 20 minutes using 40 uL of the elution buffer (150mM NaCl, 100mM Tris-HCl pH 8, 1mM EDTA, Desthiobiotin 2.5mM).

6.5 INTERACTOMIC ANALYSIS

Affinity purified samples were prepared as described in 7.4. Protein eluates were analyzed by Silver Stain to verify the enrichment of strep-tagged constructs, 4.5mg protein samples were then precipitated with Trichloroacetic acid solution 100% w/V and sent for LC-MS/MS analysis to the EdyP Service (Grenoble).

6.6 PROXIMITY BIOTINYLATION DEPENDENT (PBD) ASSAY

HEK 293T cells were transfected with the vectors pflagATG5TbID pflagATG5φdefTbID pflagTwist1TbID and pflagGFPTbID as previously described in two 10cm plates for each construct. 24 hours after transfection, biotin 500 µM in DMSO (B451, Sigma Aldrich) was added to one plate of each type, and DMSO was added to the other as a negative control. The treated cells were placed in incubation with 5% CO2 for 10 minutes. The biotinylation reaction was then stopped by placing the cell plates on ice and washing them five times with ice cold PBS. Cells were then lysed with lysis buffer (100mM NaCl, 20mM Tris-HCl pH7.5, 1% Igepal) by incubating on ice for 40 minutes. The lysate was clarified by centrifugation at 4°C for 15

minutes at 13000rpm and a portion (1%) was analyzed by western blot with α-streptavidin-HRP antibody (S911 Inviotrogen) α-Flag antibody (FG4R Invitrogen) to verify the biotinylation and flagged contructs overexpression. 20µL of Strep-Tactin resin were added to the remaining lysate and incubated at 4°C in rotation overnight. The resin was then washed 3 times with a specific washing buffer (150mM NaCl, 20mM Tris-HCl pH 7.5, 1% Igepal) and resuspended with 50µl of elution buffer (NaCl 250mM, Tris pH 7.4, 20mM, Igepal 1%, destiobiotin 2,5mM) and incubated on ice for 20 minutes. A portion of the eluted proteins was separated on SDS-PAGE and analyzed by Western blot.

6.7 WESTERN BLOT

Cells were lysed in lysis buffer (150mM NaCl, 50mM Tris-HCl pH7.5, 0.2% TritonX100, 0.3% IGEPAL, 2mM EGTA, 2mM EDTA) or the buffer reported for the specific application (AP, PBD). Samples were quantified by the Bradford method. Equal protein quantities were separated by SDS-PAGE on Criterion TGX Stain-free 4-15% gels (Biorad). Protein transfer was performed by wet blotting on a nitrocellulose membrane (Sartorius Stedim Biotech GmbH). Membranes were blocked for aspecific hybridization 1 hour at room temperature using a solution of 5% skimmed milk (AppliChem) or 5% bovine serum albumin (BSA) (fraction V, SERVA) in TBST (150Mm NaCl; Tris -HCl 10mM PH=7.5; detergent Tween® 20 0.1% w/v) based on the primary antibody used. The membranes were then incubated for 16-20 hours at 4°C with the following primary antibodies:

Sreptavidin-HRP – 1:3000 in milk, Invitrogen #S911

<u>Mouse</u>

anti-TUBULIN - 1:10.000 milk, Sigma Aldrich #0000128072; anti-FLAG – 1:1000 milk #F3165; anti-STREP – 1:1000 milk, IBA #21507001, Abcam; anti-GAPDH – 1:5000 milk, Santa Cruz #sc-32233; anti-p53- 1:1000 milk, Santa Cruz #sc-126

<u>Rabbit</u>

anti-ATG5 - 1:1000 in BSA, Cell Signaling #12994; anti-KEAP1 1:3000 in BSA, Cell Signaling #7705S; anti-NRF2 1:5000 milk, Abcam #ab137550

Primary antibodies were detected with anti-mouse/rabbit HRP-conjugated antibodies (Perkin Elmer). Blots were visualized by enhanced Chemiluminescence (Western Lightning Plus-ECL reagent, Perkin Elmer) and imaged on a Chemidoc XRS+ Imaging System (BioRad). The Image-Lab software was employed to for the densitometric analysis and image output (BioRad).

6.8 FUNCTIONAL ANNOTATION ANALYSES

The gene annotation of the non-autophagic ATG5 interaction partners identified by affinity purification coupled to LC-MS/MS as reported in Table 1 was carried out using Metascape online tool keeping default settings and analysis as species= H. Sapiens (Y. Zhou et al., 2019).

Functional annotation of RNA-Sequencing data was carried out using Gene Set Enrichment Analysis (GSEA) (Mootha et al., 2003; Subramanian et al., 2005) GSEA was run in the standard mode using the broad institute GSEA desktop app (version 4.3.2). Analysis was conducted with default options, including number of permutations=1000, enrichment statistic=weighted, metric for ranking genes=Signal2Noise. GSEA was run against a gene set downloaded from the Broad Institute Molecular Signatures Database (MSigDB v7.4) SINGH_NRF2_UP (Singh et al., 2021). Another signature (BOCCI_NAMANI_NRF2_UP) was generated from a literature dataset based on (Bocci et al., 2019; Namani et al., 2017).

7 REFERENCES

Ades, F., Zardavas, D., Bozovic-Spasojevic, I., Pugliano, L., Fumagalli, D., de Azambuja, E., Viale, G., Sotiriou, C., & Piccart, M. (2014). Luminal B breast cancer: molecular characterization, clinical management, and future perspectives. *Journal of Clinical Oncology*, *32*(25), 2794–2803. https://doi.org/10.1200/JCO.2013.54.1870

Agarwal, S., Bell, C. M., Rothbart, S. B., & Moran, R. G. (2015). AMP-activated Protein Kinase (AMPK) Control of mTORC1 Is p53- and TSC2-independent in Pemetrexed-treated Carcinoma Cells. *The Journal of Biological Chemistry*, *290*(46), 27473–27486. https://doi.org/10.1074/jbc.M115.665133

Aghdassi, A., Sendler, M., Guenther, A., Mayerle, J., Behn, C.-O., Heidecke, C.-D., Friess, H., Büchler, M., Evert, M., Lerch, M. M., & Weiss, F. U. (2012). Recruitment of histone deacetylases HDAC1 and HDAC2 by the transcriptional repressor ZEB1 downregulates E-cadherin expression in pancreatic cancer. *Gut*, *61*(3), 439–448. https://doi.org/10.1136/gutjnl-2011-300060

Aiello, N. M., Maddipati, R., Norgard, R. J., Balli, D., Li, J., Yuan, S., Yamazoe, T., Black, T., Sahmoud, A., Furth, E. E., Bar-Sagi, D., & Stanger, B. Z. (2018). EMT subtype influences epithelial plasticity and mode of cell migration. *Developmental Cell*, *45*(6), 681-695.e4. https://doi.org/10.1016/j.devcel.2018.05.027

Alanis-Lobato, G., Andrade-Navarro, M. A., & Schaefer, M. H. (2017). HIPPIE v2.0: enhancing meaningfulness and reliability of protein-protein interaction networks. *Nucleic Acids Research*, *45*(D1), D408–D414. https://doi.org/10.1093/nar/gkw985

Alexander, N. R., Tran, N. L., Rekapally, H., Summers, C. E., Glackin, C., & Heimark, R. L. (2006). N-cadherin gene expression in prostate carcinoma is modulated by integrin-dependent nuclear translocation of Twist1. *Cancer Research*, *66*(7), 3365–3369. https://doi.org/10.1158/0008-5472.CAN-05-3401

Arfmann-Knübel, S., Struck, B., Genrich, G., Helm, O., Sipos, B., Sebens, S., & Schäfer, H. (2015). The Crosstalk between Nrf2 and TGF-β1 in the Epithelial-Mesenchymal Transition of Pancreatic Duct Epithelial Cells. *Plos One*, *10*(7), e0132978. https://doi.org/10.1371/journal.pone.0132978

Baines, K., Yoshioka, K., Takuwa, Y., & Lane, J. D. (2022). The ATG5 interactome links clathrin-mediated vesicular trafficking with the autophagosome assembly machinery. *Autophagy Reports*, *1*(1), 88–118. https://doi.org/10.1080/27694127.2022.2042054

Barbazán, J., Alonso-Alconada, L., Elkhatib, N., Geraldo, S., Gurchenkov, V., Glentis, A., van Niel, G., Palmulli, R., Fernández, B., Viaño, P., Garcia-Caballero, T., López-López, R., Abal, M., & Vignjevic, D. M. (2017). Liver metastasis is facilitated by the adherence of circulating tumor cells to vascular fibronectin deposits. *Cancer Research*, *77*(13), 3431–3441. https://doi.org/10.1158/0008-5472.CAN-16-1917

Bellezza, I., Giambanco, I., Minelli, A., & Donato, R. (2018). Nrf2-Keap1 signaling in oxidative and reductive stress. *Biochimica et Biophysica Acta. Molecular Cell Research*, *1865*(5), 721–733. https://doi.org/10.1016/j.bbamcr.2018.02.010

Bialek, P., Kern, B., Yang, X., Schrock, M., Sosic, D., Hong, N., Wu, H., Yu, K., Ornitz, D. M., Olson, E. N., Justice, M. J., & Karsenty, G. (2004). A twist code determines the onset of osteoblast differentiation. *Developmental Cell*, *6*(3), 423–435. https://doi.org/10.1016/s1534-5807(04)00058-9

Bocci, F., Tripathi, S. C., Vilchez Mercedes, S. A., George, J. T., Casabar, J. P., Wong, P. K., Hanash, S. M., Levine, H., Onuchic, J. N., & Jolly, M. K. (2019). NRF2 activates a partial epithelial-mesenchymal transition and is maximally present in a hybrid epithelial/mesenchymal phenotype. *Integrative Biology: Quantitative Biosciences from Nano to Macro*, *11*(6), 251–263. https://doi.org/10.1093/intbio/zyz021

Bolós, V., Peinado, H., Pérez-Moreno, M. A., Fraga, M. F., Esteller, M., & Cano, A. (2003). The transcription factor Slug represses E-cadherin expression and induces epithelial to mesenchymal transitions: a comparison with Snail and E47 repressors. *Journal of Cell Science*, *116*(Pt 3), 499–511. https://doi.org/10.1242/jcs.00224

Brabletz, S., Schuhwerk, H., Brabletz, T., & Stemmler, M. P. (2021). Dynamic EMT: a multi-tool for tumor progression. *The EMBO Journal*, *40*(18), e108647. https://doi.org/10.15252/embj.2021108647

Bracken, C. P., Gregory, P. A., Kolesnikoff, N., Bert, A. G., Wang, J., Shannon, M. F., & Goodall, G. J. (2008). A double-negative feedback loop between ZEB1-SIP1 and the microRNA-200 family regulates epithelial-mesenchymal transition. *Cancer Research*, *68*(19), 7846–7854. https://doi.org/10.1158/0008-5472.CAN-08-1942

Burk, U., Schubert, J., Wellner, U., Schmalhofer, O., Vincan, E., Spaderna, S., & Brabletz, T. (2008). A reciprocal repression between ZEB1 and members of the miR-200 family promotes EMT and invasion in cancer cells. *EMBO Reports*, *9*(6), 582–589. https://doi.org/10.1038/embor.2008.74

Cancer Genome Atlas Network. (2012). Comprehensive molecular portraits of human breast tumours. *Nature*, *490*(7418), 61–70. https://doi.org/10.1038/nature11412

Canel, M., Serrels, A., Frame, M. C., & Brunton, V. G. (2013). E-cadherin-integrin crosstalk in cancer invasion and metastasis. *Journal of Cell Science*, *126*(Pt 2), 393–401. https://doi.org/10.1242/jcs.100115

Casas, E., Kim, J., Bendesky, A., Ohno-Machado, L., Wolfe, C. J., & Yang, J. (2011). Snail2 is an essential mediator of Twist1-induced epithelial mesenchymal transition and metastasis. *Cancer Research*, *71*(1), 245–254. https://doi.org/10.1158/0008-5472.CAN-10-2330

Changotra, H., Kaur, S., Yadav, S. S., Gupta, G. L., Parkash, J., & Duseja, A. (2022). ATG5: A central autophagy regulator implicated in various human diseases. *Cell Biochemistry and Function*, *40*(7), 650–667. https://doi.org/10.1002/cbf.3740

Chang, C., Jensen, L. E., & Hurley, J. H. (2021). Autophagosome biogenesis comes out of the black box. *Nature Cell Biology*, *23*(5), 450–456. https://doi.org/10.1038/s41556-021-00669-y

Chew, L. H., & Yip, C. K. (2014). Structural biology of the macroautophagy machinery. *Frontiers in Biology*, *9*(1), 18–34. https://doi.org/10.1007/s11515-014-1293-3

Chiang, C., & Ayyanathan, K. (2013). Snail/Gfi-1 (SNAG) family zinc finger proteins in transcription regulation, chromatin dynamics, cell signaling, development, and disease. *Cytokine & Growth Factor Reviews*, *24*(2), 123–131. https://doi.org/10.1016/j.cytogfr.2012.09.002

Chio, I. I. C., Jafarnejad, S. M., Ponz-Sarvise, M., Park, Y., Rivera, K., Palm, W., Wilson, J., Sangar, V., Hao, Y., Öhlund, D., Wright, K., Filippini, D., Lee, E. J., Da Silva, B., Schoepfer, C., Wilkinson, J. E., Buscaglia, J. M., DeNicola, G. M., Tiriac, H., … Tuveson, D. A. (2016). NRF2 Promotes Tumor Maintenance by Modulating mRNA Translation in Pancreatic Cancer. *Cell*, *166*(4), 963–976. https://doi.org/10.1016/j.cell.2016.06.056

Damiano, V., Brisotto, G., Borgna, S., di Gennaro, A., Armellin, M., Perin, T., Guardascione, M., Maestro, R., & Santarosa, M. (2017). Epigenetic silencing of miR-200c in breast cancer is associated with aggressiveness and is modulated by ZEB1. *Genes, Chromosomes & Cancer*, *56*(2), 147–158. https://doi.org/10.1002/gcc.22422

Damiano, V., Spessotto, P., Vanin, G., Perin, T., Maestro, R., & Santarosa, M. (2020). The Autophagy Machinery Contributes to E-cadherin Turnover in Breast Cancer. *Frontiers in Cell and Developmental Biology*, *8*, 545. https://doi.org/10.3389/fcell.2020.00545

Dang, T. T., Esparza, M. A., Maine, E. A., Westcott, J. M., & Pearson, G. W. (2015). ΔNp63α Promotes Breast Cancer Cell Motility through the Selective Activation of Components of the Epithelial-to-Mesenchymal Transition Program. *Cancer Research*, *75*(18), 3925–3935. https://doi.org/10.1158/0008-5472.CAN-14-3363

Dave, N., Guaita-Esteruelas, S., Gutarra, S., Frias, À., Beltran, M., Peiró, S., & de Herreros, A. G. (2011). Functional cooperation between Snail1 and twist in the regulation of ZEB1 expression during epithelial to mesenchymal transition. *The Journal of Biological Chemistry*, *286*(14), 12024–12032. https://doi.org/10.1074/jbc.M110.168625

DeNicola, G. M., Karreth, F. A., Humpton, T. J., Gopinathan, A., Wei, C., Frese, K., Mangal, D., Yu, K. H., Yeo, C. J., Calhoun, E. S., Scrimieri, F., Winter, J. M., Hruban, R. H., Iacobuzio-Donahue, C., Kern, S. E., Blair, I. A., & Tuveson, D. A. (2011). Oncogene-induced Nrf2 transcription promotes ROS detoxification and tumorigenesis. *Nature*, *475*(7354), 106–109. https://doi.org/10.1038/nature10189

Dikic, I., & Elazar, Z. (2018). Mechanism and medical implications of mammalian autophagy. *Nature Reviews. Molecular Cell Biology*, *19*(6), 349–364. https://doi.org/10.1038/s41580-018-0003-4

Dongre, A., & Weinberg, R. A. (2019). New insights into the mechanisms of epithelial-mesenchymal transition and implications for cancer. *Nature Reviews. Molecular Cell Biology*, *20*(2), 69–84. https://doi.org/10.1038/s41580-018-0080-4

Dong, P., Karaayvaz, M., Jia, N., Kaneuchi, M., Hamada, J., Watari, H., Sudo, S., Ju, J., & Sakuragi, N. (2013). Mutant p53 gain-of-function induces epithelial-mesenchymal transition through modulation of the miR-130b-ZEB1 axis. *Oncogene*, *32*(27), 3286–3295. https://doi.org/10.1038/onc.2012.334

Dooley, H. C., Razi, M., Polson, H. E. J., Girardin, S. E., Wilson, M. I., & Tooze, S. A. (2014). WIPI2 links LC3 conjugation with PI3P, autophagosome formation, and pathogen clearance by recruiting Atg12-5-16L1. *Molecular Cell*, *55*(2), 238–252. https://doi.org/10.1016/j.molcel.2014.05.021

Feng, Y., He, D., Yao, Z., & Klionsky, D. J. (2014). The machinery of macroautophagy. *Cell Research*, *24*(1), 24–41. https://doi.org/10.1038/cr.2013.168

Fernández-Albarral, J. A., de Julián-López, E., Soler-Domínguez, C., de Hoz, R., López-Cuenca, I., Salobrar-García, E., Ramírez, J. M., Pinazo-Durán, M. D., Salazar, J. J., & Ramírez, A. I. (2021). The role of autophagy in eye diseases. *Life (Basel, Switzerland)*, *11*(3). https://doi.org/10.3390/life11030189

Fimia, G. M., Stoykova, A., Romagnoli, A., Giunta, L., Di Bartolomeo, S., Nardacci, R., Corazzari, M., Fuoco, C., Ucar, A., Schwartz, P., Gruss, P., Piacentini, M., Chowdhury, K., & Cecconi, F. (2007). Ambra1 regulates autophagy and development of the nervous system. *Nature*, *447*(7148), 1121–1125. https://doi.org/10.1038/nature05925

Fu, J., Qin, L., He, T., Qin, J., Hong, J., Wong, J., Liao, L., & Xu, J. (2011). The TWIST/Mi2/NuRD protein complex and its essential role in cancer metastasis. *Cell Research*, *21*(2), 275–289. https://doi.org/10.1038/cr.2010.118

Galluzzi, L., & Green, D. R. (2019). Autophagy-Independent Functions of the Autophagy Machinery. *Cell*, *177*(7), 1682–1699. https://doi.org/10.1016/j.cell.2019.05.026

Gatica, D., Lahiri, V., & Klionsky, D. J. (2018). Cargo recognition and degradation by selective autophagy. *Nature Cell Biology*, *20*(3), 233–242. https://doi.org/10.1038/s41556-018-0037-z

Gazinska, P., Grigoriadis, A., Brown, J. P., Millis, R. R., Mera, A., Gillett, C. E., Holmberg, L. H., Tutt, A. N., & Pinder, S. E. (2013). Comparison of basal-like triple-negative breast cancer defined by morphology, immunohistochemistry and transcriptional profiles. *Modern Pathology*, *26*(7), 955–966. https://doi.org/10.1038/modpathol.2012.244

Gonzalez-Angulo, A. M., Timms, K. M., Liu, S., Chen, H., Litton, J. K., Potter, J., Lanchbury, J. S., Stemke-Hale, K., Hennessy, B. T., Arun, B. K., Hortobagyi, G. N., Do, K.-A., Mills, G. B., & Meric-Bernstam, F. (2011). Incidence and outcome of BRCA mutations in unselected patients with triple receptor-negative breast cancer. *Clinical Cancer Research*, *17*(5), 1082–1089. https://doi.org/10.1158/1078-0432.CCR-10-2560

Grandvallet, C., Feugeas, J. P., Monnien, F., Despouy, G., Valérie, P., Michaël, G., Hervouet, E., & Peixoto, P. (2020). Autophagy is associated with a robust specific transcriptional signature in breast cancer subtypes. *Genes & Cancer*, *11*(3–4), 154–168. https://doi.org/10.18632/genesandcancer.208

Grosse-Wilde, A., Fouquier d'Hérouël, A., McIntosh, E., Ertaylan, G., Skupin, A., Kuestner, R. E., del Sol, A., Walters, K.-A., & Huang, S. (2015). Stemness of the hybrid Epithelial/Mesenchymal State in Breast Cancer and Its Association with Poor Survival. *Plos One*, *10*(5), e0126522. https://doi.org/10.1371/journal.pone.0126522

Grumati, P., Morozzi, G., Hölper, S., Mari, M., Harwardt, M.-L. I., Yan, R., Müller, S., Reggiori, F., Heilemann, M., & Dikic, I. (2017). Full length RTN3 regulates turnover of tubular endoplasmic reticulum via selective autophagy. *ELife*, *6*. https://doi.org/10.7554/eLife.25555

Gugnoni, M., Sancisi, V., Manzotti, G., Gandolfi, G., & Ciarrocchi, A. (2016). Autophagy and epithelial-mesenchymal transition: an intricate interplay in cancer. *Cell Death & Disease*, *7*(12), e2520. https://doi.org/10.1038/cddis.2016.415

Guo, H., Sadoul, R., & Gibbings, D. (2018). Autophagy-independent effects of autophagy-related-5 (Atg5) on exosome production and metastasis. *Molecular & Cellular Oncology*, *5*(3), e1445941. https://doi.org/10.1080/23723556.2018.1445941

Guo, J. Y., Xia, B., & White, E. (2013). Autophagy-mediated tumor promotion. *Cell*, *155*(6), 1216–1219. https://doi.org/10.1016/j.cell.2013.11.019

Gupta, P. B., Pastushenko, I., Skibinski, A., Blanpain, C., & Kuperwasser, C. (2019). Phenotypic plasticity: driver of cancer initiation, progression, and therapy resistance. *Cell Stem Cell*, *24*(1), 65–78. https://doi.org/10.1016/j.stem.2018.11.011

Hajra, K. M., Chen, D. Y.-S., & Fearon, E. R. (2002). The SLUG zinc-finger protein represses E-cadherin in breast cancer. *Cancer Research*, *62*(6), 1613–1618.

Haller, M., Hock, A. K., Giampazolias, E., Oberst, A., Green, D. R., Debnath, J., Ryan, K. M., Vousden, K. H., & Tait, S. W. G. (2014). Ubiquitination and proteasomal degradation of ATG12 regulates its proapoptotic activity. *Autophagy*, *10*(12), 2269–2278. https://doi.org/10.4161/15548627.2014.981914

Hamacher-Brady, A., Brady, N. R., Logue, S. E., Sayen, M. R., Jinno, M., Kirshenbaum, L. A., Gottlieb, R. A., & Gustafsson, A. B. (2007). Response to myocardial ischemia/reperfusion injury involves Bnip3 and autophagy. *Cell Death and Differentiation*, *14*(1), 146–157. https://doi.org/10.1038/sj.cdd.4401936

Hamamori, Y., Wu, H. Y., Sartorelli, V., & Kedes, L. (1997). The basic domain of myogenic basic helix-loop-helix (bHLH) proteins is the novel target for direct inhibition by another bHLH protein, Twist. *Molecular and Cellular Biology*, *17*(11), 6563–6573. https://doi.org/10.1128/MCB.17.11.6563

Harada, K., Miyake, H., Kusuda, Y., & Fujisawa, M. (2012). Expression of epithelial-mesenchymal transition markers in renal cell carcinoma: impact on prognostic outcomes in patients undergoing radical nephrectomy. *BJU International*, *110*(11 Pt C), E1131-7. https://doi.org/10.1111/j.1464-410X.2012.11297.x

Hosokawa, N., Hara, T., Kaizuka, T., Kishi, C., Takamura, A., Miura, Y., Iemura, S., Natsume, T., Takehana, K., Yamada, N., Guan, J.-L., Oshiro, N., & Mizushima, N. (2009). Nutrient-dependent mTORC1 association with the ULK1-Atg13-FIP200 complex required for autophagy. *Molecular Biology of the Cell*, *20*(7), 1981–1991. https://doi.org/10.1091/mbc.E08-12-1248

Huang, Y., Hong, W., & Wei, X. (2022). The molecular mechanisms and therapeutic strategies of EMT in tumor progression and metastasis. *Journal of Hematology & Oncology*, *15*(1), 129. https://doi.org/10.1186/s13045-022-01347-8

Hu, W.-H., Yang, W.-C., Liu, P.-F., Liu, T.-T., Morgan, P., Tsai, W.-L., Pan, H.-W., Lee, C.-H., & Shu, C.-W. (2021). Clinicopathological Association of Autophagy Related 5 Protein with Prognosis of Colorectal Cancer. *Diagnostics (Basel)*, *11*(5). https://doi.org/10.3390/diagnostics11050782

Itakura, E., & Mizushima, N. (2010). Characterization of autophagosome formation site by a hierarchical analysis of mammalian Atg proteins. *Autophagy*, *6*(6), 764–776. https://doi.org/10.4161/auto.6.6.12709

Ivanov, A. I., & Naydenov, N. G. (2013). Dynamics and regulation of epithelial adherens junctions: recent discoveries and controversies. *International Review of Cell and Molecular Biology*, *303*, 27–99. https://doi.org/10.1016/B978-0-12-407697-6.00002-7

Kalluri, R., & Weinberg, R. A. (2009). The basics of epithelial-mesenchymal transition. *The Journal of Clinical Investigation*, *119*(6), 1420–1428. https://doi.org/10.1172/JCI39104

Kaushik, S., & Cuervo, A. M. (2018). The coming of age of chaperone-mediated autophagy. *Nature Reviews. Molecular Cell Biology*, *19*(6), 365–381. https://doi.org/10.1038/s41580-018-0001-6

Khaminets, A., Heinrich, T., Mari, M., Grumati, P., Huebner, A. K., Akutsu, M., Liebmann, L., Stolz, A., Nietzsche, S., Koch, N., Mauthe, M., Katona, I., Qualmann, B., Weis, J., Reggiori, F., Kurth, I., Hübner, C. A., & Dikic, I. (2015). Regulation of endoplasmic reticulum turnover by selective autophagy. *Nature*, *522*(7556), 354–358. https://doi.org/10.1038/nature14498

Kim, J., Yang, C., Kim, E. J., Jang, J., Kim, S.-J., Kang, S. M., Kim, M. G., Jung, H., Park, D., & Kim, C. (2016). Vimentin filaments regulate integrin-ligand interactions by binding to the cytoplasmic tail of integrin β3. *Journal of Cell Science*, *129*(10), 2030–2042. https://doi.org/10.1242/jcs.180315

Kim, N. H., Kim, H. S., Li, X.-Y., Lee, I., Choi, H.-S., Kang, S. E., Cha, S. Y., Ryu, J. K., Yoon, D., Fearon, E. R., Rowe, R. G., Lee, S., Maher, C. A., Weiss, S. J., & Yook, J. I. (2011). A p53/miRNA-34 axis regulates Snail1-dependent cancer cell epithelial-mesenchymal transition. *The Journal of Cell Biology*, *195*(3), 417–433. https://doi.org/10.1083/jcb.201103097

Komatsu, M., Kurokawa, H., Waguri, S., Taguchi, K., Kobayashi, A., Ichimura, Y., Sou, Y.-S., Ueno, I., Sakamoto, A., Tong, K. I., Kim, M., Nishito, Y., Iemura, S., Natsume, T., Ueno, T., Kominami, E., Motohashi, H., Tanaka, K., & Yamamoto,

M. (2010). The selective autophagy substrate p62 activates the stress responsive transcription factor Nrf2 through inactivation of Keap1. *Nature Cell Biology*, *12*(3), 213–223. https://doi.org/10.1038/ncb2021

Ko, E., Kim, D., Min, D. W., Kwon, S.-H., & Lee, J.-Y. (2021). Nrf2 regulates cell motility through RhoA-ROCK1 signalling in non-small-cell lung cancer cells. *Scientific Reports*, *11*(1), 1247. https://doi.org/10.1038/s41598-021-81021-0

Krebs, A. M., Mitschke, J., Lasierra Losada, M., Schmalhofer, O., Boerries, M., Busch, H., Boettcher, M., Mougiakakos, D., Reichardt, W., Bronsert, P., Brunton, V. G., Pilarsky, C., Winkler, T. H., Brabletz, S., Stemmler, M. P., & Brabletz, T. (2017). The EMT-activator Zeb1 is a key factor for cell plasticity and promotes metastasis in pancreatic cancer. *Nature Cell Biology*, *19*(5), 518–529. https://doi.org/10.1038/ncb3513

Kreike, B., van Kouwenhove, M., Horlings, H., Weigelt, B., Peterse, H., Bartelink, H., & van de Vijver, M. J. (2007). Gene expression profiling and histopathological characterization of triple-negative/basal-like breast carcinomas. *Breast Cancer Research*, *9*(5), R65. https://doi.org/10.1186/bcr1771

Kröger, C., Afeyan, A., Mraz, J., Eaton, E. N., Reinhardt, F., Khodor, Y. L., Thiru, P., Bierie, B., Ye, X., Burge, C. B., & Weinberg, R. A. (2019). Acquisition of a hybrid E/M state is essential for tumorigenicity of basal breast cancer cells. *Proceedings of the National Academy of Sciences of the United States of America*, *116*(15), 7353–7362. https://doi.org/10.1073/pnas.1812876116

Kuburich, N. A., den Hollander, P., Pietz, J. T., & Mani, S. A. (2022). Vimentin and cytokeratin: Good alone, bad together. *Seminars in Cancer Biology*, *86*(Pt 3), 816–826. https://doi.org/10.1016/j.semcancer.2021.12.006

Kuma, A., Hatano, M., Matsui, M., Yamamoto, A., Nakaya, H., Yoshimori, T., Ohsumi, Y., Tokuhisa, T., & Mizushima, N. (2004). The role of autophagy during the early neonatal starvation period. *Nature*, *432*(7020), 1032–1036. https://doi.org/10.1038/nature03029

Kuo, J.-C. (2014). Focal adhesions function as a mechanosensor. *Progress in Molecular Biology and Translational Science*, *126*, 55–73. https://doi.org/10.1016/B978-0-12-394624-9.00003-8

Kvokačková, B., Remšík, J., Jolly, M. K., & Souček, K. (2021). Phenotypic Heterogeneity of Triple-Negative Breast Cancer Mediated by Epithelial-Mesenchymal Plasticity. *Cancers*, *13*(9). https://doi.org/10.3390/cancers13092188

Lamark, T., & Johansen, T. (2021). Mechanisms of selective autophagy. *Annual Review of Cell and Developmental Biology*, *37*, 143–169. https://doi.org/10.1146/annurev-cellbio-120219-035530

Lambertini, M., Ceppi, M., Poggio, F., Peccatori, F. A., Azim, H. A., Ugolini, D., Pronzato, P., Loibl, S., Moore, H. C. F., Partridge, A. H., Bruzzi, P., & Del Mastro, L. (2015). Ovarian suppression using luteinizing hormone-releasing hormone agonists during chemotherapy to preserve ovarian function and fertility of breast cancer patients: a meta-analysis of randomized studies. *Annals of Oncology*, *26*(12), 2408–2419. https://doi.org/10.1093/annonc/mdv374

Lehmann, B. D., Bauer, J. A., Chen, X., Sanders, M. E., Chakravarthy, A. B., Shyr, Y., & Pietenpol, J. A. (2011). Identification of human triple-negative breast cancer subtypes and preclinical models for selection of targeted therapies. *The Journal of Clinical Investigation*, *121*(7), 2750–2767. https://doi.org/10.1172/JCI45014

Lesurf, R., Griffith, O. L., Griffith, M., Hundal, J., Trani, L., Watson, M. A., Aft, R., Ellis, M. J., Ota, D., Suman, V. J., Meric-Bernstam, F., Leitch, A. M., Boughey, J. C., Unzeitig, G., Buzdar, A. U., Hunt, K. K., & Mardis, E. R. (2017). Genomic characterization of HER2-positive breast cancer and response to neoadjuvant trastuzumab and chemotherapy-results from the ACOSOG Z1041 (Alliance) trial. *Annals of Oncology*, *28*(5), 1070–1077. https://doi.org/10.1093/annonc/mdx048

Levine, B., & Kroemer, G. (2019). Biological functions of autophagy genes: A disease perspective. *Cell*, *176*(1–2), 11–42. https://doi.org/10.1016/j.cell.2018.09.048

Lignitto, L., LeBoeuf, S. E., Homer, H., Jiang, S., Askenazi, M., Karakousi, T. R., Pass, H. I., Bhutkar, A. J., Tsirigos, A., Ueberheide, B., Sayin, V. I., Papagiannakopoulos, T., & Pagano, M. (2019). Nrf2 activation promotes lung cancer metastasis by inhibiting the degradation of bach1. *Cell*, *178*(2), 316-329.e18. https://doi.org/10.1016/j.cell.2019.06.003

Lim, S., Becker, A., Zimmer, A., Lu, J., Buettner, R., & Kirfel, J. (2013). SNAI1-mediated epithelial-mesenchymal transition confers chemoresistance and cellular plasticity by regulating genes involved in cell death and stem cell maintenance. *Plos One*, *8*(6), e66558. https://doi.org/10.1371/journal.pone.0066558

Lin, T.-Y., Chan, H.-H., Chen, S.-H., Sarvagalla, S., Chen, P.-S., Coumar, M. S., Cheng, S. M., Chang, Y.-C., Lin, C.-H., Leung, E., & Cheung, C. H. A. (2020). BIRC5/Survivin is a novel ATG12-ATG5 conjugate interactor and an autophagy-induced DNA damage suppressor in human cancer and mouse embryonic fibroblast cells. *Autophagy*, *16*(7), 1296–1313. https://doi.org/10.1080/15548627.2019.1671643

Liu, H., Wang, C., Yi, F., Yeo, S., Haas, M., Tang, X., & Guan, J.-L. (2021). Non-canonical function of FIP200 is required for neural stem cell maintenance and differentiation by limiting TBK1 activation and p62 aggregate formation. *Scientific Reports*, *11*(1), 23907. https://doi.org/10.1038/s41598-021-03404-7

Li, S., Zhang, L., Zhang, G., Shangguan, G., Hou, X., Duan, W., Xi, Y., Xu, N., Zhang, B., Dong, J., Wang, Y., Cui, W., & Chen, S. (2021). A nonautophagic role of ATG5 in regulating cell growth by targeting c-Myc for proteasome-mediated degradation. *IScience*, *24*(11), 103296. https://doi.org/10.1016/j.isci.2021.103296

Li, W., Li, J., & Bao, J. (2012). Microautophagy: lesser-known self-eating. *Cellular and Molecular Life Sciences*, *69*(7), 1125–1136. https://doi.org/10.1007/s00018-011-0865-5

Li, X., He, S., & Ma, B. (2020). Autophagy and autophagy-related proteins in cancer. *Molecular Cancer*, *19*(1), 12. https://doi.org/10.1186/s12943-020-1138-4

Luck, K., Kim, D.-K., Lambourne, L., Spirohn, K., Begg, B. E., Bian, W., Brignall, R., Cafarelli, T., Campos-Laborie, F. J., Charloteaux, B., Choi, D., Coté, A. G., Daley, M., Deimling, S., Desbuleux, A., Dricot, A., Gebbia, M., Hardy, M. F., Kishore, N., … Calderwood, M. A. (2020). A reference map of the human binary protein interactome. *Nature*, *580*(7803), 402–408. https://doi.org/10.1038/s41586-020-2188-x

Maskey, D., Yousefi, S., Schmid, I., Zlobec, I., Perren, A., Friis, R., & Simon, H.-U. (2013). ATG5 is induced by DNA-damaging agents and promotes mitotic catastrophe independent of autophagy. *Nature Communications*, *4*, 2130. https://doi.org/10.1038/ncomms3130

Matoba, K., Kotani, T., Tsutsumi, A., Tsuji, T., Mori, T., Noshiro, D., Sugita, Y., Nomura, N., Iwata, S., Ohsumi, Y., Fujimoto, T., Nakatogawa, H., Kikkawa, M., & Noda, N. N. (2020). Atg9 is a lipid scramblase that mediates autophagosomal membrane expansion. *Nature Structural & Molecular Biology*, *27*(12), 1185–1193. https://doi.org/10.1038/s41594-020-00518-w

Matsumoto, A., Jinno, H., Murata, T., Seki, T., Takahashi, M., Hayashida, T., Kameyama, K., & Kitagawa, Y. (2015). Prognostic implications of receptor discordance between primary and recurrent breast cancer. *International Journal of Clinical Oncology / Japan Society of Clinical Oncology*, *20*(4), 701–708. https://doi.org/10.1007/s10147-014-0759-2

Melia, T. J., Lystad, A. H., & Simonsen, A. (2020). Autophagosome biogenesis: From membrane growth to closure. *The Journal of Cell Biology*, *219*(6). https://doi.org/10.1083/jcb.202002085

Menegon, S., Columbano, A., & Giordano, S. (2016). The dual roles of NRF2 in cancer. *Trends in Molecular Medicine*, *22*(7), 578–593. https://doi.org/10.1016/j.molmed.2016.05.002

Mizushima, N, Sugita, H., Yoshimori, T., & Ohsumi, Y. (1998). A new protein conjugation system in human. The counterpart of the yeast Apg12p conjugation system essential for autophagy. *The Journal of Biological Chemistry*, *273*(51), 33889–33892. https://doi.org/10.1074/jbc.273.51.33889

Mizushima, Noboru, & Komatsu, M. (2011). Autophagy: renovation of cells and tissues. *Cell*, *147*(4), 728–741. https://doi.org/10.1016/j.cell.2011.10.026

Mizushima, Noboru, Yoshimori, T., & Ohsumi, Y. (2011). The role of Atg proteins in autophagosome formation. *Annual Review of Cell and Developmental Biology*, *27*, 107–132. https://doi.org/10.1146/annurev-cellbio-092910-154005

Moes, M., Le Béchec, A., Crespo, I., Laurini, C., Halavatyi, A., Vetter, G., Del Sol, A., & Friederich, E. (2012). A novel network integrating a miRNA-203/SNAI1 feedback loop which regulates epithelial to mesenchymal transition. *Plos One*, *7*(4), e35440. https://doi.org/10.1371/journal.pone.0035440

Molina, M. A., Codony-Servat, J., Albanell, J., Rojo, F., Arribas, J., & Baselga, J. (2001). Trastuzumab (herceptin), a humanized anti-Her2 receptor monoclonal antibody, inhibits basal and activated Her2 ectodomain cleavage in breast cancer cells. *Cancer Research*, *61*(12), 4744–4749.

Montagner, M., Bhome, R., Hooper, S., Chakravarty, P., Qin, X., Sufi, J., Bhargava, A., Ratcliffe, C. D. H., Naito, Y., Pocaterra, A., Tape, C. J., & Sahai, E. (2020). Crosstalk with lung epithelial cells regulates Sfrp2-mediated latency in breast cancer dissemination. *Nature Cell Biology*, *22*(3), 289–296. https://doi.org/10.1038/s41556-020-0474-3

Mootha, V. K., Lindgren, C. M., Eriksson, K.-F., Subramanian, A., Sihag, S., Lehar, J., Puigserver, P., Carlsson, E., Ridderstråle, M., Laurila, E., Houstis, N., Daly, M. J., Patterson, N., Mesirov, J. P., Golub, T. R., Tamayo, P., Spiegelman, B., Lander, E. S., Hirschhorn, J. N., … Groop, L. C. (2003). PGC-1alpha-responsive genes involved in oxidative phosphorylation are coordinately downregulated in human diabetes. *Nature Genetics*, *34*(3), 267–273. https://doi.org/10.1038/ng1180

Namani, A., Cui, Q. Q., Wu, Y., Wang, H., Wang, X. J., & Tang, X. (2017). NRF2-regulated metabolic gene signature as a prognostic biomarker in non-small cell lung cancer. *Oncotarget*, *8*(41), 69847–69862. https://doi.org/10.18632/oncotarget.19349

Nieto, M A, Sargent, M. G., Wilkinson, D. G., & Cooke, J. (1994). Control of cell behavior during vertebrate development by Slug, a zinc finger gene. *Science*, *264*(5160), 835–839. https://doi.org/10.1126/science.7513443

Nieto, M Angela, Huang, R. Y.-J., Jackson, R. A., & Thiery, J. P. (2016). EMT: 2016. *Cell*, *166*(1), 21–45. https://doi.org/10.1016/j.cell.2016.06.028

Orrantia-Borunda, E., Anchondo-Nuñez, P., Acuña-Aguilar, L. E., Gómez-Valles, F. O., & Ramírez-Valdespino, C. A. (2022). Subtypes of breast cancer. In H. N. Mayrovitz (Ed.), *Breast Cancer*. Exon Publications. https://doi.org/10.36255/exon-publications-breast-cancer-subtypes

Otomo, C., Metlagel, Z., Takaesu, G., & Otomo, T. (2013). Structure of the human ATG12~ATG5 conjugate required for LC3 lipidation in autophagy. *Nature Structural & Molecular Biology*, *20*(1), 59–66. https://doi.org/10.1038/nsmb.2431

Oughtred, R., Rust, J., Chang, C., Breitkreutz, B.-J., Stark, C., Willems, A., Boucher, L., Leung, G., Kolas, N., Zhang, F., Dolma, S., Coulombe-Huntington, J., Chatr-Aryamontri, A., Dolinski, K., & Tyers, M. (2021). The BioGRID database: A comprehensive biomedical resource of curated protein, genetic, and chemical interactions. *Protein Science*, *30*(1), 187–200. https://doi.org/10.1002/pro.3978

Pankiv, S., Clausen, T. H., Lamark, T., Brech, A., Bruun, J.-A., Outzen, H., Øvervatn, A., Bjørkøy, G., & Johansen, T. (2007). p62/SQSTM1 binds directly to Atg8/LC3 to facilitate degradation of ubiquitinated protein aggregates by autophagy. *The Journal of Biological Chemistry*, *282*(33), 24131–24145. https://doi.org/10.1074/jbc.M702824200

Park, S.-M., Gaur, A. B., Lengyel, E., & Peter, M. E. (2008). The miR-200 family determines the epithelial phenotype of cancer cells by targeting the E-cadherin repressors ZEB1 and ZEB2. *Genes & Development*, *22*(7), 894–907. https://doi.org/10.1101/gad.1640608

Pastushenko, I., Brisebarre, A., Sifrim, A., Fioramonti, M., Revenco, T., Boumahdi, S., Van Keymeulen, A., Brown, D., Moers, V., Lemaire, S., De Clercq, S., Minguijón, E., Balsat, C., Sokolow, Y., Dubois, C., De Cock, F., Scozzaro, S., Sopena, F., Lanas, A., … Blanpain, C. (2018). Identification of the tumour transition states occurring during EMT. *Nature*, *556*(7702), 463–468. https://doi.org/10.1038/s41586-018-0040-3

Pastushenko, I., Mauri, F., Song, Y., de Cock, F., Meeusen, B., Swedlund, B., Impens, F., Van Haver, D., Opitz, M., Thery, M., Bareche, Y., Lapouge, G., Vermeersch, M., Van Eycke, Y.-R., Balsat, C., Decaestecker, C., Sokolow, Y., Hassid, S., Perez-Bustillo, A., … Blanpain, C. (2021). Fat1 deletion promotes hybrid EMT state, tumour stemness and metastasis. *Nature*, *589*(7842), 448–455. https://doi.org/10.1038/s41586-020-03046-1

Piccinin, S., Tonin, E., Sessa, S., Demontis, S., Rossi, S., Pecciarini, L., Zanatta, L., Pivetta, F., Grizzo, A., Sonego, M., Rosano, C., Dei Tos, A. P., Doglioni, C., & Maestro, R. (2012). A "twist box" code of p53 inactivation: twist box: p53 interaction promotes p53 degradation. *Cancer Cell*, *22*(3), 404–415. https://doi.org/10.1016/j.ccr.2012.08.003

Pillai, R., Hayashi, M., Zavitsanou, A.-M., & Papagiannakopoulos, T. (2022). NRF2: keaping tumors protected. *Cancer Discovery*, *12*(3), 625–643. https://doi.org/10.1158/2159-8290.CD-21-0922

Puisieux, A., Brabletz, T., & Caramel, J. (2014). Oncogenic roles of EMT-inducing transcription factors. *Nature Cell Biology*, *16*(6), 488–494. https://doi.org/10.1038/ncb2976

Puram, S. V., Tirosh, I., Parikh, A. S., Patel, A. P., Yizhak, K., Gillespie, S., Rodman, C., Luo, C. L., Mroz, E. A., Emerick, K. S., Deschler, D. G., Varvares, M. A., Mylvaganam, R., Rozenblatt-Rosen, O., Rocco, J. W., Faquin, W. C., Lin, D. T., Regev, A., & Bernstein, B. E. (2017). Single-Cell Transcriptomic Analysis of Primary and Metastatic Tumor Ecosystems in Head and Neck Cancer. *Cell*, *171*(7), 1611-1624.e24. https://doi.org/10.1016/j.cell.2017.10.044

Qiang, L., Zhao, B., Ming, M., Wang, N., He, T.-C., Hwang, S., Thorburn, A., & He, Y.-Y. (2014). Regulation of cell proliferation and migration by p62 through stabilization of Twist1. *Proceedings of the National Academy of Sciences of the United States of America*, *111*(25), 9241–9246. https://doi.org/10.1073/pnas.1322913111

Reggiori, F., & Klionsky, D. J. (2013). Autophagic processes in yeast: mechanism, machinery and regulation. *Genetics*, *194*(2), 341–361. https://doi.org/10.1534/genetics.112.149013

Rick, J. W., Chandra, A., Dalle Ore, C., Nguyen, A. T., Yagnik, G., & Aghi, M. K. (2019). Fibronectin in malignancy: Cancer-specific alterations, protumoral effects, and therapeutic implications. *Seminars in Oncology*, *46*(3), 284–290. https://doi.org/10.1053/j.seminoncol.2019.08.002

Rojo de la Vega, M., Chapman, E., & Zhang, D. D. (2018). NRF2 and the hallmarks of cancer. *Cancer Cell*, *34*(1), 21–43. https://doi.org/10.1016/j.ccell.2018.03.022

Rolland, T., Taşan, M., Charloteaux, B., Pevzner, S. J., Zhong, Q., Sahni, N., Yi, S., Lemmens, I., Fontanillo, C., Mosca, R., Kamburov, A., Ghiassian, S. D., Yang, X., Ghamsari, L., Balcha, D., Begg, B. E., Braun, P., Brehme, M., Broly, M. P., … Vidal, M. (2014). A proteome-scale map of the human interactome network. *Cell*, *159*(5), 1212–1226. https://doi.org/10.1016/j.cell.2014.10.050

Saini, M., Schmidleitner, L., Moreno, H. D., Donato, E., Falcone, M., Bartsch, J. M., Klein, C., Vogel, V., Würth, R., Pfarr, N., Espinet, E., Lehmann, M., Königshoff, M., Reitberger, M., Haas, S., Graf, E., Schwarzmayr, T., Strom, T.-M., Spaich, S., … Scheel, C. H. (2023). Resistance to mesenchymal reprogramming sustains clonal propagation in metastatic breast cancer. *Cell Reports*, 112533. https://doi.org/10.1016/j.celrep.2023.112533

Sakuma, Y., Nishikiori, H., Hirai, S., Yamaguchi, M., Yamada, G., Watanabe, A., Hasegawa, T., Kojima, T., Niki, T., & Takahashi, H. (2016). Prolyl isomerase Pin1 promotes survival in EGFR-mutant lung adenocarcinoma cells with an epithelial-mesenchymal transition phenotype. *Laboratory Investigation*, *96*(4), 391–398. https://doi.org/10.1038/labinvest.2015.155

Sánchez-Tilló, E., Lázaro, A., Torrent, R., Cuatrecasas, M., Vaquero, E. C., Castells, A., Engel, P., & Postigo, A. (2010). ZEB1 represses E-cadherin and induces an EMT by recruiting the SWI/SNF chromatin-remodeling protein BRG1. *Oncogene*, *29*(24), 3490–3500. https://doi.org/10.1038/onc.2010.102

Santarosa, M., & Maestro, R. (2021). The Autophagic Route of E-Cadherin and Cell Adhesion Molecules in Cancer Progression. *Cancers*, *13*(24). https://doi.org/10.3390/cancers13246328

Satyavarapu, E. M., Das, R., Mandal, C., Mukhopadhyay, A., & Mandal, C. (2018). Autophagy-independent induction of LC3B through oxidative stress reveals its non-canonical role in anoikis of ovarian cancer cells. *Cell Death & Disease*, *9*(10), 934. https://doi.org/10.1038/s41419-018-0989-8

Sharabi, A. B., Aldrich, M., Sosic, D., Olson, E. N., Friedman, A. D., Lee, S.-H., & Chen, S.-Y. (2008). Twist-2 controls myeloid lineage development and function. *PLoS Biology*, *6*(12), e316. https://doi.org/10.1371/journal.pbio.0060316

Shin, H. R., & Zoncu, R. (2020). The lysosome at the intersection of cellular growth and destruction. *Developmental Cell*, *54*(2), 226–238. https://doi.org/10.1016/j.devcel.2020.06.010

Shiota, M., Izumi, H., Onitsuka, T., Miyamoto, N., Kashiwagi, E., Kidani, A., Hirano, G., Takahashi, M., Naito, S., & Kohno, K. (2008). Twist and p53 reciprocally regulate target genes via direct interaction. *Oncogene*, *27*(42), 5543–5553. https://doi.org/10.1038/onc.2008.176

Shi, Y., Sawada, J., Sui, G., Affar, E. B., Whetstine, J. R., Lan, F., Ogawa, H., Luke, M. P.-S., Nakatani, Y., & Shi, Y. (2003). Coordinated histone modifications mediated by a CtBP co-repressor complex. *Nature*, *422*(6933), 735–738. https://doi.org/10.1038/nature01550

Siemens, H., Jackstadt, R., Hünten, S., Kaller, M., Menssen, A., Götz, U., & Hermeking, H. (2011). miR-34 and SNAIL form a double-negative feedback loop to regulate epithelial-mesenchymal transitions. *Cell Cycle*, *10*(24), 4256–4271. https://doi.org/10.4161/cc.10.24.18552

Singh, A., Daemen, A., Nickles, D., Jeon, S.-M., Foreman, O., Sudini, K., Gnad, F., Lajoie, S., Gour, N., Mitzner, W., Chatterjee, S., Choi, E.-J., Ravishankar, B., Rappaport, A., Patil, N., McCleland, M., Johnson, L., Acquaah-Mensah, G., Gabrielson, E., … Hatzivassiliou, G. (2021). NRF2 Activation Promotes Aggressive Lung Cancer and Associates with Poor Clinical Outcomes. *Clinical Cancer Research*, *27*(3), 877–888. https://doi.org/10.1158/1078-0432.CCR-20-1985

Skrypek, N., Goossens, S., De Smedt, E., Vandamme, N., & Berx, G. (2017). Epithelial-to-Mesenchymal Transition: Epigenetic Reprogramming Driving Cellular Plasticity. *Trends in Genetics*, *33*(12), 943–959. https://doi.org/10.1016/j.tig.2017.08.004

Sørlie, T., Perou, C. M., Tibshirani, R., Aas, T., Geisler, S., Johnsen, H., Hastie, T., Eisen, M. B., van de Rijn, M., Jeffrey, S. S., Thorsen, T., Quist, H., Matese, J. C., Brown, P. O., Botstein, D., Lønning, P. E., & Børresen-Dale, A. L. (2001). Gene expression patterns of breast carcinomas distinguish tumor subclasses with clinical implications. *Proceedings of the National Academy of Sciences of the United States of America*, *98*(19), 10869–10874. https://doi.org/10.1073/pnas.191367098

Spada, S., Tocci, A., Di Modugno, F., & Nisticò, P. (2021). Fibronectin as a multiregulatory molecule crucial in tumor matrisome: from structural and functional features to clinical practice in oncology. *Journal of Experimental & Clinical Cancer Research*, *40*(1), 102. https://doi.org/10.1186/s13046-021-01908-8

Spicer, D. B., Rhee, J., Cheung, W. L., & Lassar, A. B. (1996). Inhibition of myogenic bHLH and MEF2 transcription factors by the bHLH protein Twist. *Science*, *272*(5267), 1476–1480. https://doi.org/10.1126/science.272.5267.1476

Stemmler, M. P., Eccles, R. L., Brabletz, S., & Brabletz, T. (2019). Non-redundant functions of EMT transcription factors. *Nature Cell Biology*, *21*(1), 102–112. https://doi.org/10.1038/s41556-018-0196-y

Subramanian, A., Tamayo, P., Mootha, V. K., Mukherjee, S., Ebert, B. L., Gillette, M. A., Paulovich, A., Pomeroy, S. L., Golub, T. R., Lander, E. S., & Mesirov, J. P. (2005). Gene set enrichment analysis: a knowledge-based approach for interpreting genome-wide expression profiles. *Proceedings of the National Academy of Sciences of the United States of America*, *102*(43), 15545–15550. https://doi.org/10.1073/pnas.0506580102

Sung, H., Ferlay, J., Siegel, R. L., Laversanne, M., Soerjomataram, I., Jemal, A., & Bray, F. (2021). Global cancer statistics 2020: GLOBOCAN estimates of incidence and mortality worldwide for 36 cancers in 185 countries. *CA: A Cancer Journal for Clinicians*, *71*(3), 209–249. https://doi.org/10.3322/caac.21660

Sun, S.-Y., Hu, X.-T., Yu, X.-F., Zhang, Y.-Y., Liu, X.-H., Liu, Y.-H., Wu, S.-H., Li, Y.-Y., Cui, S.-X., & Qu, X.-J. (2021). Nuclear translocation of ATG5 induces DNA mismatch repair deficiency (MMR-D)/microsatellite instability (MSI) via interacting with Mis18α in colorectal cancer. *British Journal of Pharmacology*, *178*(11), 2351–2369. https://doi.org/10.1111/bph.15422

Tanida, I., Ueno, T., & Kominami, E. (2004). LC3 conjugation system in mammalian autophagy. *The International Journal of Biochemistry & Cell Biology*, *36*(12), 2503–2518. https://doi.org/10.1016/j.biocel.2004.05.009

Tsang, J. Y. S., & Tse, G. M. (2020). Molecular classification of breast cancer. *Advances in Anatomic Pathology*, *27*(1), 27–35. https://doi.org/10.1097/PAP.0000000000000232

Tutt, A., Tovey, H., Cheang, M. C. U., Kernaghan, S., Kilburn, L., Gazinska, P., Owen, J., Abraham, J., Barrett, S., Barrett-Lee, P., Brown, R., Chan, S., Dowsett, M., Flanagan, J. M., Fox, L., Grigoriadis, A., Gutin, A., Harper-Wynne, C., Hatton, M. Q., … Bliss, J. M. (2018). Carboplatin in BRCA1/2-mutated and triple-negative breast cancer BRCAness subgroups: the TNT Trial. *Nature Medicine*, *24*(5), 628–637. https://doi.org/10.1038/s41591-018-0009-7

van Roy, F. (2014). Beyond E-cadherin: roles of other cadherin superfamily members in cancer. *Nature Reviews. Cancer*, *14*(2), 121–134. https://doi.org/10.1038/nrc3647

Velichkova, M., & Hasson, T. (2003). Keap1 in adhesion complexes. *Cell Motility and the Cytoskeleton*, *56*(2), 109–119. https://doi.org/10.1002/cm.10138

Velichkova, M., & Hasson, T. (2005). Keap1 regulates the oxidation-sensitive shuttling of Nrf2 into and out of the nucleus via a Crm1-dependent nuclear export mechanism. *Molecular and Cellular Biology*, *25*(11), 4501–4513. https://doi.org/10.1128/MCB.25.11.4501-4513.2005

Vera-Ramirez, L. (2020). Cell-intrinsic survival signals. The role of autophagy in metastatic dissemination and tumor cell dormancy. *Seminars in Cancer Biology*, *60*, 28–40. https://doi.org/10.1016/j.semcancer.2019.07.027

Vesuna, F., van Diest, P., Chen, J. H., & Raman, V. (2008). Twist is a transcriptional repressor of E-cadherin gene expression in breast cancer. *Biochemical and Biophysical Research Communications*, *367*(2), 235–241. https://doi.org/10.1016/j.bbrc.2007.11.151

Vilchez Mercedes, S. A., Bocci, F., Ahmed, M., Eder, I., Zhu, N., Levine, H., Onuchic, J. N., Jolly, M. K., & Wong, P. K. (2022). Nrf2 modulates the hybrid epithelial/mesenchymal phenotype and notch signaling during collective cancer migration. *Frontiers in Molecular Biosciences*, *9*, 807324. https://doi.org/10.3389/fmolb.2022.807324

Waks, A. G., & Winer, E. P. (2019). Breast cancer treatment: A review. *The Journal of the American Medical Association*, *321*(3), 288–300. https://doi.org/10.1001/jama.2018.19323

Weigelt, B., Mackay, A., A'hern, R., Natrajan, R., Tan, D. S. P., Dowsett, M., Ashworth, A., & Reis-Filho, J. S. (2010). Breast cancer molecular profiling with single sample predictors: a retrospective analysis. *The Lancet Oncology*, *11*(4), 339–349. https://doi.org/10.1016/S1470-2045(10)70008-5

White, E. (2012). Deconvoluting the context-dependent role for autophagy in cancer. *Nature Reviews. Cancer*, *12*(6), 401–410. https://doi.org/10.1038/nrc3262

Wible, D. J., Chao, H.-P., Tang, D. G., & Bratton, S. B. (2019). ATG5 cancer mutations and alternative mRNA splicing reveal a conjugation switch that regulates ATG12-ATG5-ATG16L1 complex assembly and autophagy. *Cell Discovery*, *5*, 42. https://doi.org/10.1038/s41421-019-0110-1

Wong, S.-W., Sil, P., & Martinez, J. (2018). Rubicon: LC3-associated phagocytosis and beyond. *The FEBS Journal*, *285*(8), 1379–1388. https://doi.org/10.1111/febs.14354

Wu, W.-S., You, R.-I., Cheng, C.-C., Lee, M.-C., Lin, T.-Y., & Hu, C.-T. (2017). Snail collaborates with EGR-1 and SP-1 to directly activate transcription of MMP 9 and ZEB1. *Scientific Reports*, *7*(1), 17753. https://doi.org/10.1038/s41598-017-18101-7

Xu, C., Zang, Y., Zhao, Y., Cui, W., Zhang, H., Zhu, Y., & Xu, M. (2021). Comprehensive Pan-Cancer Analysis Confirmed That ATG5 Promoted the Maintenance of Tumor Metabolism and the Occurrence of Tumor Immune Escape. *Frontiers in Oncology*, *11*, 652211. https://doi.org/10.3389/fonc.2021.652211

Yang, A., Herter-Sprie, G., Zhang, H., Lin, E. Y., Biancur, D., Wang, X., Deng, J., Hai, J., Yang, S., Wong, K.-K., & Kimmelman, A. C. (2018). Autophagy Sustains Pancreatic Cancer Growth through Both Cell-Autonomous and Nonautonomous Mechanisms. *Cancer Discovery*, *8*(3), 276–287. https://doi.org/10.1158/2159-8290.CD-17-0952

Yang, C., Cao, M., Liu, Y., He, Y., Du, Y., Zhang, G., & Gao, F. (2019). Inducible formation of leader cells driven by CD44 switching gives rise to collective invasion and metastases in luminal breast carcinomas. *Oncogene*, *38*(46), 7113–7132. https://doi.org/10.1038/s41388-019-0899-y

Yim, W. W.-Y., & Mizushima, N. (2020). Lysosome biology in autophagy. *Cell Discovery*, *6*(1), 6. https://doi.org/10.1038/s41421-020-0141-7

Yin, L., Duan, J.-J., Bian, X.-W., & Yu, S.-C. (2020). Triple-negative breast cancer molecular subtyping and treatment progress. *Breast Cancer Research*, *22*(1), 61. https://doi.org/10.1186/s13058-020-01296-5

Yousefi, S., Perozzo, R., Schmid, I., Ziemiecki, A., Schaffner, T., Scapozza, L., Brunner, T., & Simon, H.-U. (2006). Calpain-mediated cleavage of Atg5 switches autophagy to apoptosis. *Nature Cell Biology*, *8*(10), 1124–1132. https://doi.org/10.1038/ncb1482

Yuan, H.-X., Russell, R. C., & Guan, K.-L. (2013). Regulation of PIK3C3/VPS34 complexes by MTOR in nutrient stress-induced autophagy. *Autophagy*, *9*(12), 1983–1995. https://doi.org/10.4161/auto.26058

Yu, L., McPhee, C. K., Zheng, L., Mardones, G. A., Rong, Y., Peng, J., Mi, N., Zhao, Y., Liu, Z., Wan, F., Hailey, D. W., Oorschot, V., Klumperman, J., Baehrecke, E. H., & Lenardo, M. J. (2010). Termination of autophagy and reformation of lysosomes regulated by mTOR. *Nature*, *465*(7300), 942–946. https://doi.org/10.1038/nature09076

Zeisberg, M., & Neilson, E. G. (2009). Biomarkers for epithelial-mesenchymal transitions. *The Journal of Clinical Investigation*, *119*(6), 1429–1437. https://doi.org/10.1172/JCI36183

Zhang, Z., Qu, J., Zheng, C., Zhang, P., Zhou, W., Cui, W., Mo, X., Li, L., Xu, L., & Gao, J. (2018). Nrf2 antioxidant pathway suppresses Numb-mediated epithelial-mesenchymal transition during pulmonary fibrosis. *Cell Death & Disease*, *9*(2), 83. https://doi.org/10.1038/s41419-017-0198-x

Zheng, X., Carstens, J. L., Kim, J., Scheible, M., Kaye, J., Sugimoto, H., Wu, C.-C., LeBleu, V. S., & Kalluri, R. (2015). Epithelial-to-mesenchymal transition is dispensable for metastasis but induces chemoresistance in pancreatic cancer. *Nature*, *527*(7579), 525–530. https://doi.org/10.1038/nature16064

Zhou, S., Wang, X., Ding, J., Yang, H., & Xie, Y. (2021). Increased ATG5 expression predicts poor prognosis and promotes EMT in cervical carcinoma. *Frontiers in Cell and Developmental Biology*, *9*, 757184. https://doi.org/10.3389/fcell.2021.757184

Zhou, W., Mo, X., Cui, W., Zhang, Z., Li, D., Li, L., Xu, L., Yao, H., & Gao, J. (2016). Nrf2 inhibits epithelial-mesenchymal transition by suppressing snail expression during pulmonary fibrosis. *Scientific Reports*, *6*, 38646. https://doi.org/10.1038/srep38646

Zhou, Y., Zhou, B., Pache, L., Chang, M., Khodabakhshi, A. H., Tanaseichuk, O., Benner, C., & Chanda, S. K. (2019). Metascape provides a biologist-oriented resource for the analysis of systems-level datasets. *Nature Communications*, *10*(1), 1523. https://doi.org/10.1038/s41467-019-09234-6

8 ACKNOWLEDGMENTS

This work was possible thanks to the collaboration with Yohann Couté, Sabine Brugière and Lucid Belmudes from the EDyP Lab (Institut de Recherche Interdisciplinaire de Grenoble).

I would like to thank Dr. Roberta Maestro for her guidance and scientific advice. I would like to thank Dr. Manuela Santarosa who made it possible for me to realize this work by giving me time and patience and sharing her knowledge with me.
I would also like to thank Dr. Valentina Damiano, who laid the foundation for this research and guided me during the first year of my PhD, and Dr. Arianna Ortolano, who contributed to the experiments during her Master's internship.
I would like to thank Dr. Sara Piccinin and Flavia Pivetta for their advice and suggestions on the experimental procedures and their fundamental support in carrying out the wet lab work.
I am also very grateful to all the people I met during these three years in the Oncogenetics and Functional Oncogenomics Unit and at the CRO National Cancer Institute. In particular, I am grateful to those among them who have become dear friends sharing daily joys and sorrows of research and private life.
I would like to thank my PhD partner in crime Dr. Ilaria de Benedictis, who helped me overcome the most difficult moments by pushing me with optimism and fortitude.

Finally, I cannot forget to thank my family, Massimo and all my friends for the support they have given me during these three challenging years.